Scientia Chromatographica 2016; 8(4):239-256
Instituto Internacional de Cromatografia
http://dx.doi.org/10.4322/sc.2016.036
ISSN 1984-4433

Extração em Fase Sólida Magnética (MSPE): Fundamentos e Aplicações

Magnetic Solid Phase Extraction (MSPE): Fundamentals and Applications

Amandha Kaiser da Silva[1]
Eduardo Sobieski Neto[1]
Luiz Henrique Viana[1]
Fernando Mauro Lanças[2]
Carlos Eduardo Domingues Nazario[1*]

[1]Instituto de Química, Universidade Federal de Mato Grosso do Sul, Campo Grande, MS, Brasil
[2]Instituto de Química de São Carlos, Universidade de São Paulo, São Carlos, SP, Brasil
*carlos.nazario@ufms.br

Recebido: 01-11-2016
Aceito: 02-12-2016

Resumo

Diversas estratégias de preparo de amostras têm sido desenvolvidas com o objetivo de diminuir a tempo de análise e a manipulação da amostra, e maximizar a pré-concentração dos analitos em matrizes complexas. O uso da tecnologia de separação magnética tem se destacado para esta finalidade pela simplificação das etapas de preparo de amostra. Neste conceito, a extração em fase sólida magnética (MSPE) baseia-se na manipulação de nanopartículas magnéticas para promover a separação das fases. Além da simplicidade e alta eficiência de extração, a MSPE supera alguns inconvenientes da SPE e d-SPE convencional. Nesta revisão, são discutidos os conceitos e estratégias de síntese das partículas magnéticas modificadas com diversos recobrimentos (sílica, MIP, surfactantes, líquidos iônicos, grafeno e derivados) para a extração e pré-concentração dos analitos em diversas matrizes.

Palavras-chave: preparo de amostra, MSPE, nanopartículas magnéticas, análise de traços.

Abstract

Several sample preparation strategies have been developed in order to decrease the analysis time and sample manipulation, and to maximize the analytes preconcentration in complex matrices. The use of magnetic separation technology has been highlighted for this purpose by the simplification of the sample preparation steps. In this concept, the magnetic solid phase extraction (MSPE) is based on the manipulation of magnetic nanoparticles to promote phase separation. In addition to simplicity and high extraction efficiency, the MSPE overcomes some drawbacks of conventional SPE and d-SPE. In this review, the authors discuss the concepts and strategies to prepare magnetic particles modified with different coatings (silica, MIP, surfactants, ionic liquids, graphene and derivatives) for the extraction and preconcentration of the analytes in several matrices.

Keywords: sample preparation, MSPE, magnetic nanoparticles, trace analysis.

1. Introdução

A alta complexidade das matrizes juntamente com a baixa concentração dos analitos tem exigido um árduo trabalho de manipulação da amostra antes da análise instrumental (cromatografia líquida, cromatografia gasosa, espectroscopia atômica e espectrometria de massas)[1]. Além dessa vertente ser tediosa, pode influenciar negativamente na precisão e exatidão do método analítico. Dessa forma, diminuir o número de etapas no preparo de amostra sem reduzir a eficiência de extração é um desafio constante aos pesquisadores.

Desde a introdução da extração em fase sólida (SPE) na década de 1970, o uso de técnicas de extração baseada em sorbentes tem se destacado pela possibilidade de aumentar a seletividade dentro do preceito de química verde. Uma das variações da SPE, a extração em fase sólida dispersiva (*dispersive solid phase extraction*, d-SPE) possui como grande vantagem a redução do tempo de preparo de amostra[2]. Diferentemente da SPE, no qual o sorbente está empacotado no cartucho, a fase extratora da d-SPE é adicionada diretamente na matriz para extração/*clean-up* dos analitos. Assim, o contato imediato entre as fases proporciona uma extração mais efetiva sem a necessidade de pré-condicionar cartuchos ou a demora na percolação de grande volume de amostra.

Após atingir o tempo de equilíbrio na extração, a separação do sorbente e da matriz na d-SPE pode ser realizado por (a) centrifugação, (b) filtração ou (c) separação magnética. Essa última estratégia tem recebido enorme atenção dos pesquisadores nos últimos anos pois simplifica o processo de extração pela manipulação de um campo magnético externo.

Nanopartículas magnéticas (*magnetic nanoparticles*, MNPs) são os sorbentes utilizados nessa estratégia de preparo de amostra no qual são um grupo de partículas dentro da área de nanomateriais que possuem escala nanométrica com propriedades superparamagnética. De maneira geral, as partículas são fortemente atraídas por um campo magnético externo. Entretanto, quando o campo magnético é removido, as partículas não retêm magnetismo residual[3].

Normalmente as MNPs são compostas por um núcleo rígido com propriedade magnética recoberta por uma camada de polímero que fornece a seletividade necessária para a extração dos analitos. É usual utilizar a terminologia "núcleo magnético@recobrimento" para facilitar a exemplificação do referido material de extração (Figura 1). Por exemplo, um material magnético no qual possui o núcleo baseado em óxido de ferro (Fe_3O_4) recoberto com sílica (SiO_2) e funcionalizado com o grupamento C18 pode ser representado como Fe_3O_4@ SiO_2-C18.

O uso de MNPs em preparo de amostra ganhou destaque no ano de 1996 com o trabalho publicado por Towler et al.[5] no qual utilizaram Fe_3O_4@MnO_2 para a extração de metais em água do mar. Após três anos, o termo extração em fase sólida magnética (*magnetic solid phase extraction*, m-SPE ou MSPE) foi introduzido por Safarikova and Safarik[6] na extração de compostos orgânicos com estrutura planar (corante trifenilmetano, hidrocarbonetos poliaromáticos e alguns derivados). Como resultado, as MNPs (Fe_3O_4@SiO_2-NH_2-ftalocianina de cobre) promoveram um fator de enriquecimento em torno de 460 vezes.

Em comparação à SPE e d-SPE convencional, algumas aplicações da MSPE utilizam pequena quantidade de fase extratora (10–50 mg). Assim, os termos microextração em fase sólida magnética

Figura 1. Imagem de microscopia eletrônica de transmissão (TEM) da (a) MNP de Fe_3O_4 e (b) MNP recoberta com sílica (Fe_3O_4@SiO_2). Adaptado com permissão da ref (4). Copyright (2008) American Chemical Society.

(*magnetic-micro-SPE*, m-μ-SPE) ou microextração em fase sólida magnética dispersiva (*magnetic dispersive micro-SPE*, m-d-μ-SPE) também são comumente encontrados na literatura.

O fato de utilizar as propriedades magnéticas para separar a fase extratora da matriz analítica, na MSPE não há necessidade de centrífugas ou sistemas de filtração no processo de extração. Assim, o tempo de preparo de amostra e a perda de analitos são minimizados. Outras vantagens, tais como, a pequena quantidade de fase extratora, o baixo consumo de solvente orgânico, a reutilização do sorbentes e a possibilidade de projetar a seletividade do sorbentes também tem sido relatadas ao uso de MNPs.

A Figura 2 demonstra a representação esquemática da MSPE. Na primeira etapa ocorre a dispersão do sorbentes na matriz líquida para a extração dos analitos. Após atingir o tempo de equilíbrio, um magneto (imã) é utilizado para separar a matriz da fase extratora. Por fim, os analitos são eluidos em um solvente adequado e conduzidos para análise instrumental. O uso de agitação mecânica, vortex ou o uso de ultrassom nas etapas de extração/*clean up* são comumente utilizadas para facilitar a dispersão das MNPs.

É importante ressaltar que muitos materiais baseados em nanopartículas (NPs) tem sido aplicados em métodos de preparo de amostra. Contudo, iremos centralizar nossa discussão apenas nas NPs com propriedades magnéticas.

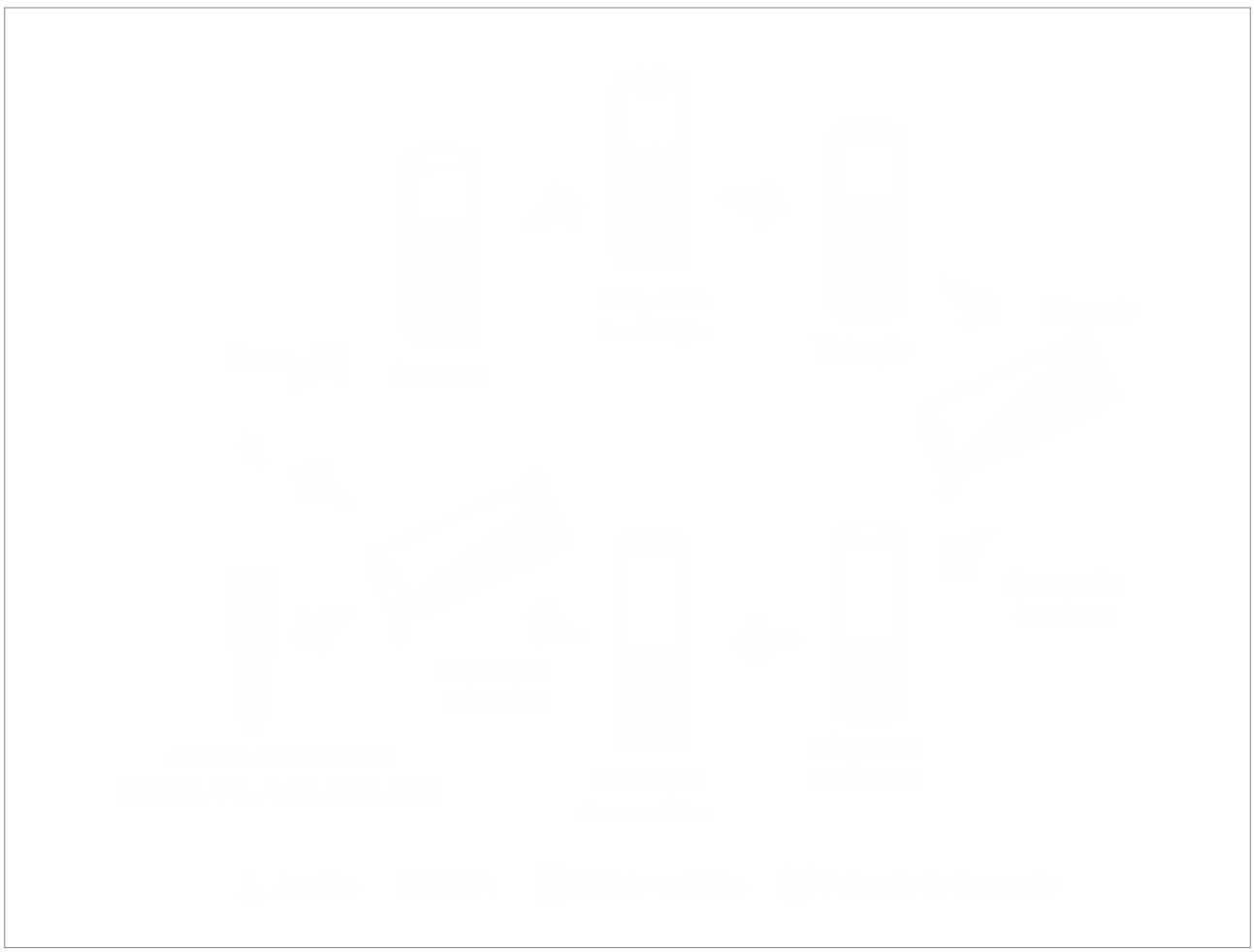

Figura 2. Representação esquemática das etapas da extração em fase sólida magnética (MSPE). Adaptado com permissão da ref. (2). Copyright (2015) John Wiley and Sons Inc.

2. Propriedades das MNPs e seus métodos de síntese

MNPs são aglomerados com uma dimensão característica na ordem de nanômetros (10^{-9} m) as quais possuem propriedades físicas e químicas diferenciadas e dependentes do tamanho, morfologia e estrutura cristalina[7]. Nas últimas décadas, houve um crescente interesse investigativo para compreensão de suas propriedades, estrutura e toxicidade devido a aplicação em diversas áreas (industrial, biomédica e separações).

Até o momento, poucas informações estão disponíveis sobre a toxicidade das MNPs. O tamanho nanométrico pode representar um risco aos seres humanos e ao meio ambiente, pois são capazes de penetrar nas células de maneira facilitada e diferenciada em relação a partículas maiores. É de conhecimento que à toxicidade das NPs é potencializada pelo método de fabricação, armazenamento, transporte e pela maneira na qual são incorporadas em produtos comercializados. Assim, sem as medidas de proteção, esses materiais podem ser inalados nos locais de trabalho (incluindo laboratórios de pesquisa), além da possível exposição dérmica em quantidades significativas. Em contato com o ser humano, as NPs podem danificar as células pela liberação de radicais livres a uma dose que supera as defesas naturais do organismo. Quanto ao impacto ambiental, atualmente poucas evidências são encontradas pela dificuldade de avaliação sobre a toxicidade em espécies não humanas, assim como os riscos de bioacumulação[8].

Na literatura são encontrados vários tipos de MNPs, tais como: óxidos de ferro (Fe_3O_4, γ-Fe_2O_3, α-Fe_2O_3, entre outros); ferritas de Co, Ni e Mg; e FePt, Co, Fe, Ni, CoPt, FeCo. Contudo, apenas as MNPs de óxido de ferro são aprovadas pela *U.S Food and Drug Admistration* (F.D.A) devido a sua biocompatibilidade com materiais orgânicos conferindo-as um grande potencial de aplicação área industrial, medicinal e ambiental. Adicionalmente, os materiais baseados em óxido de ferro são quimicamente inertes, possuem baixa toxicidade e várias opções para síntese e modificação de sua superfície[9].

A literatura descreve uma dificuldade de distinção entre os óxidos de ferro devido à similaridade das partículas por não serem monocristais[9]. Desse modo, a caracterização das MNPs é comumente realizada através das técnicas de difração de raios X (XRD), microscopia eletrônica de transmissão (TEM) ou microscopia eletrônica de varredura (SEM). Enquanto pela XRD é possível determinar a estrutura química da MNP, a TEM e SEM são usadas para o estudo das suas características morfológicas[10].

Entre os 16 tipos de óxidos de ferro conhecidos, incluindo os hidróxidos e óxi-hidróxidos de ferro[11], a hematita (α-Fe_2O_3), magnetita (Fe_3O_4) e maghemita (γ-Fe_2O_3) são as MNPs comumente utilizadas devido aos seus polimorfismos, no qual a transição de fases ocorre pela indução da temperatura[12]. Apesar da mesma fórmula molecular, a hematita e maghemita diferem pelas suas estruturas cristalinas. A hematita possui célula unitária com simetria hexagonal com pares de $Fe(O)_6$ octaedros devido ao arranjo dos cátions. Na maghemita, a célula unitária é cúbica e a maioria dos cátions presentes são de Fe(III). A diferença da magnetita em relação aos demais óxidos consiste na presença de ambos íons Fe(III) e Fe(II) podendo escrever sua fórmula como $Y[XY]O_4$ (X = Fe(II) e Y = Fe(III)). A célula unitária é do tipo cúbica de face-centrada e sua estrutura cristalina consiste em camadas octaédricas e camadas mistas tetraédrica/octaédrica empilhadas[11]. Os íons Fe(II) estão presentes na metade da camada octaédrica e os íons Fe(III) ocupam uniformemente a camada mista octaédrica/tetraédrica[12].

Muitos elementos de transição e/ou seus óxidos podem apresentar propriedades magnéticas, as quais são classificadas em dois tipos: substâncias que possuem momento de dipolo magnético atômico finito diferente de zero ($\mu_{at} \neq 0$) e substâncias que possuem $\mu_{at} = 0$. O primeiro grupo compreende os materiais paramagnéticos com ordenamento ferromagnético, antiferromagnético ou ferrimagnético dos dipolos. O

segundo grupo corresponde aos materiais diamagnéticos no qual o momento de dipolo magnético é igual a zero (não magnéticos). Como as propriedades magnéticas de partículas com $\mu_{at} \neq 0$ são fortemente dependentes de sua geometria e dimensão, o óxido de ferro nanocristalino apresenta comportamento superparamagnético, enquanto sua escala micrométrica possui comportamento ferrimagnético. O termo superparamagnetismo está relacionado ao estudo das propriedades magnéticas de um único domínio magnético (monodomínio) com sistema análogo ao paramagnetismo[7].

Entre as estratégias para confirmação do comportamento superparamagnético de um sistema pode-se destacar: (a) a plotagem do gráfico magnetização reduzida *versus* campo magnético em determinada temperatura resulta na curva ideal conhecida como "lei de escala clássica do superparamagnetismo"; (b) se as isotermas de magnetização são de histerese; e (c) se a distribuição de tamanho ajustada é independente da temperatura[13].

Em relação a síntese, atualmente, diversas metodologias para preparo de MNPs baseadas em óxido de ferro têm sido desenvolvidas e, entre as mais comuns, pode-se citar os métodos de coprecipitação, síntese hidrotérmica e solvotérmica, sol-gel, decomposição térmica, microemulsão, e síntese sonoquímica. O desenvolvimento destas metodologias tem a preocupação sobre o escalonamento de produção e o controle das características das partículas, tais como a cristalinidade, estabilidade química, tamanho e estrutura. Estas características influenciam nas propriedades magnéticas das partículas e podem ser ajustadas através do controle das condições reacionais (pH, velocidade de agitação e temperatura de reação)[14].

O método clássico e usual para a obtenção de Fe_3O_4 ou γ-Fe_2O_3 é a coprecipitação no qual consiste na adição de uma solução alcalina em uma solução aquosa de Fe(II) e Fe(III) na proporção molar de 1:2 sob temperatura ambiente ou com aquecimento[14]. A reação pode ser exemplificada de acordo com a Equação 1[12].

$$Fe^{2+} + 2\,Fe^{3+} + 8\,OH^- \leftrightarrows Fe(OH)_2 + 2\,Fe(OH)_3 \rightarrow Fe_3O_4 \downarrow + 4\,H_2O \quad (1)$$

Devido ao fato das MNPs de Fe_3O_4 serem facilmente oxidadas para Fe_2O_3 na presença de oxigênio (O_2), o meio reacional deve ser realizado sob atmosfera inerte. O controle do tamanho e da estrutura das NPs é realizado através da variação da velocidade de agitação, concentração e tipo de base empregada, do sal de ferro utilizado e da temperatura da reação. Uma característica desse método é a obtenção de partículas com baixa cristalinidade e ampla faixa de distribuição de tamanho. Além disso, o uso de alto valor de pH na mistura reacional pode auxiliar na obtenção de MNPs uniformes e monodispersas[14]. A maioria dos trabalhos envolvendo MNPs aplicadas em preparo de amostra utilizam o método de coprecipitação para a síntese do núcleo magnético (Fe_3O_4) dos sorbentes.

Tradicionalmente, após a solubilização dos cloretos de Fe(II) e Fe(III) em meio aquoso, ocorre a adição de amônia à temperatura de 75ºC-90ºC sob atmosfera inerte para a formação das MNPs[15,16]. Entretanto, variações sintéticas são relatadas na literatura, tais como o uso de sulfato de Fe(II) como substituinte do cloreto de Fe(II)[17-19], hidróxido de sódio utilizado como base[17,19] e reações realizadas à temperatura ambiente[18,19]. E Rajput et al.[20] ainda relata a adição hidróxido de tetrametilamônio após a lavagem como prevenção da formação de aglomerados.

Uma alternativa sintética é o método hidrotérmico no qual inclui várias tecnologias químicas via úmida para cristalização de substâncias em recipiente fechado. Essa cristalização ocorre a partir da alta temperatura de uma solução aquosa (130ºC - 250ºC) e alta pressão de vapor (0,3 - 4 MPa). Essa síntese tende a fornecer MNPs de óxidos de ferro com alta cristalinidade. Adicionalmente, essa metodologia possui a capacidade de criar fases cristalinas que não são estáveis no ponto de fusão[12], e também pode ser usada no preparo de nanoestruturas incomuns de óxidos de ferros (nanotubos e esferas ocas)[14].

A diferença entre o método hidrotérmico e o solvotérmico consiste na utilização de solução aquosa e solução não-aquosa, respectivamente, no processo de cristalização. Ambas as rotas sintéticas são utilizadas para obtenção de NPs de α-Fe_2O_3, γ-Fe_2O_3 e Fe_3O_4 com alta cristalinidade[12]. Bao et al.[21] seguiu este método para a síntese da MNPs de Fe_3O_4 o qual dissolveu cloreto férrico, citrato sódio e acetato de sódio em etileno glicol. A amostra foi aquecida à 200ºC e em seguida arrefecida à temperatura ambiente.

O método sol-gel refere-se a hidrólise e condensação dos alcóxidos metálicos os quais conduzem as dispersões estáveis de partículas coloidais (sol) de óxido catalisada por ácidos ou bases. O tipo de catalizador utilizado tem influência na característica final do gel (maior ou menor ramificação)[22]. A reação pode ser conduzida a temperatura ambiente ou com aquecimento e tratamentos térmicos são necessários para a obtenção do estado cristalino final. As MNPs de óxidos de ferro são formadas por uma transformação de fases de dois passos ($Fe(OH)_3 \rightarrow \beta$-FeOOH $\rightarrow \gamma$-Fe_2O_3). As propriedades das NPs são dependentes da estrutura criada durante o estado sol do processo sol-gel[12].

As vantagens dessa estratégia em relação ao método de coprecipitação consiste na dispersão em solventes polares (aquoso ou orgânico) devido à presença de ligantes hidrofílicos na superfície das NPs. Adicionalmente, o uso de temperatura no processo de síntese favorece a cristalinidade e magnetização saturada. Como desvantagem, pode-se citar o alto custo dos precursores alcóxidos metálicos e a necessidade de uma etapa de calcinação[12,22]. Zhang et al.[23] avaliou a influência das estruturas cristalinas dos óxidos de ferro na adsorção de metais pesados. Os óxidos foram preparados pelo método sol-gel via micelas induzidas por dodecil sulfato de sódio (SDS). Posteriormente, na etapa de calcinação, foi avaliado a estrutura dos óxidos de acordo com a temperatura utilizada. Observou-se que o aumento da temperatura de calcinação (200ºC, 350ºC e 500ºC) transformou o óxido de ferro amorfo (Fe_3O_4) em ($\alpha + \gamma$)-Fe_2O_3 e na estrutura com alto grau de cristalização (α-Fe_2O_3). Além disso, a área de superfície e o volume dos poros destes óxidos diminuíram. É importante ressaltar que a estrutura amorfa do Fe_3O_4 apresentou maior capacidade de adsorção para Pb(II) e Cd(II) em relação às outras duas estruturas.

O método de preparo das NPs conhecido como decomposição térmica tem como princípio da técnica o uso de temperatura elevada para decompor os precursores organometálicos ou complexos metálicos. Os precursores ($[Fe(CO)_5]$, $[Fe(acac)_3]$, ferro oleato, $[Fe(cup)_3]$, ferroceno $[Fe(C_5H_5)_2]$) são solubilizados em solventes orgânicos de alto ponto de ebulição na presença de surfactantes (os ácido oleico, ácido graxo, 1-octadeceno, oleilamina e hexadecilamina). De modo geral, os precursores podem ser introduzidos no meio reacional já aquecido, ou a mistura, incluindo o precursor, é preparada a temperatura ambiente com posterior aquecimento em sistema aberto ou fechado.

Outra característica importante está relacionada ao número de etapas da síntese: se o precursor possui metal de valência zero, é possível preparar NPs através de duas etapas; contudo, na decomposição de precursores metálicos catiônicos ocorre a formação do óxido em uma única etapa. Por exemplo, γ-Fe_2O_3 pode ser obtido através da decomposição térmica de $[Fe(CO)_5]$ dissolvendo-o em uma mistura de octil éter e ácido oleico na primeira etapa, e adicionando um fraco oxidante na segunda etapa. Enquanto que Fe_3O_4 pode ser obtido em uma única etapa pela decomposição térmica do $[Fe(acac)_3]$ em 1,2-hexadecanediol, oleilamina e ácido oleico em fenol éter. As condições reacionais (proporção dos reagente, surfactante e solvente, temperatura, tempo de reação e tempo de envelhecimento) são importantes para o controle do tamanho e morfologia das MNPs. Embora esse método tenha a vantagem da obtenção de partículas esféricas (ou cúbicas) monodispersas de óxido de ferro com diâmetro inferior a 30 nm, a desvantagem é a solubilização dessas NPs em solventes apolares[12,14,24].

A metodologia de microemulsão consiste na dispersão dos precursores em dois líquidos imiscíveis (sistema água e óleo), no qual são estabilizados por uma película interfacial formada por moléculas do surfactante. Nesse sistema, a fase aquosa contém os sais metálicos enquanto a fase lipofílica é formada por uma mistura complexa de diferentes hidrocarbonetos e olefinas.

As microemulsões podem ser classificadas em direta (óleo disperso na água) ou reversa (água dispersa no óleo). Na microemulsão direta, a fase aquosa é dispersa como micropartículas, geralmente entre 1 a 50 nm de diâmentro, sobre a monocamada do surfactante sob a fase orgânica. O tamanho da micela reversa é determinado pela razão molar entre a água e o surfactante. Através da mistura de duas microemulsões (reversa) idênticas contendo os reagentes desejados, as micropartículas se colidem continuamente, aglutinam e se quebram novamente formando, finalmente, o precipitado em micelas.

Com a adição de solventes, como acetona ou etanol, o precipitado obtido nessa metodologia pode ser extraído da mistura por filtragem ou centrifugação. Apesar da presença de surfactantes, devido a agregação na produção das NPMs, geralmente, são necessários vários processos de lavagem e tratamentos de estabilização. Os surfactantes comumente usados neste caso são: bis(2-etilhexil)sulfocianeto, dodecil sulfato de sódio (SDS) e brometo de cetiltrimetilamonio (CTAB). O tamanho e a formação das NPMs podem ser comumente controlados através da variação da concentração dos reagentes e a natureza dos surfactantes. Contudo, quando comparado com a coprecipitação e decomposição térmica, essa metodologia possui baixo rendimento e grandes quantidades de solventes são necessárias para a obtenção de uma quantidade considerável do material[12,14,24].

Por fim, a síntese sonoquímica consiste na utilização de efeitos químicos de ultrassom decorrente da cavitação acústica. Perante a radiação de ultrassom, a alternação entre expansão e compressão das ondas acústicas criam cavidades que podem acumular energia. A liberação desta energia provoca uma implosão nas cavidades gerando temperatura de 5000 K, pressão de aproximadamente 1800 bar e taxa de resfriamento acima de 1010 Ks^{-1}. Através dessa metodologia, MNPs de magnetita podem ser sintetizadas pela sonicação de acetato de Fe(II) em água sob atmosfera de argônio. As vantagens do uso da síntese sonoquímica no preparo de MNPs estão relacionadas ao fato de ser uma síntese rápida, sem elevação da temperatura ou pressão, e com preceitos de química verde[12,14].

3. Recobrimento das MNPs

As MNPs geralmente são recobertas devido à instabilidade que este tipo de material pode apresentar, sendo vulneráveis a oxidações e com tendência a formação de aglomerados[25]. Adicionalmente, os recobrimentos também auxiliam na modificação da seletividade do sorbentes no processo de extração[26,27]. Por esta razão, o número de trabalhos aplicados em preparo de amostra que não utilizam a etapa de recobrimento das NPMs são reduzidos.

Os recobrimentos dos núcleos das MNPs podem ser realizados com materiais inorgânicos, orgânicos ou híbridos através de ligações química ou interações físicas. Para designar o recobrimento mais adequado, é importante considerar a natureza de interação analito-sorbente.

Com uma grande vantagem em relação aos demais materiais, a sílica é o sorbente mais utilizado em separações analíticas devido ao fato de possuir um custo relativamente baixo, ser quimicamente inerte, ter boa estabilidade térmica, elevada área superficial e apresentar tamanho e poros uniformes[10,28]. A maioria dos trabalhos que utilizam recobrimento das MNPs com sílica ($Fe_3O_4@SiO_2$) fazem uso do método de sol-gel[29] ou microemulsão (micela reversa)[10], mas outras metodologias também podem ser utilizadas[30-32].

O recobrimento pelo método sol-gel ocorre pelas reações de hidrólise e condensação dos precursores de sílica (alcoxissilano ou sal de silicato) na presença de

um solvente e um catalisador (ácido ou base). O ajuste das condições reacionais é determinante para controlar a espessura da camada de sílica na MNPs[33-35]. Na síntese pelo método de microemulsão, as MNPs são dispersas em um solvente contendo água, óleo e surfactante para formar uma emulsão. O surfactante utilizado necessita apresentar baixa tensão superficial entre a água e o óleo formando uma solução transparente. Deve-se utilizar surfactantes específicos como por exemplo o AOT[36], Brij-07 ou Triton X-100[37]. Uma das vantagens desse método consiste no fato do revestimento de sílica uniforme ser sintetizado sem aglomeração dos grupos[38].

Os recobrimentos com precursores de sílica (Fe_3O_4@SiO_2) possuem grupos silanois (Si-OH) na superfície do material que possibilitam a posterior funcionalização com diversos grupos químicos promovendo extrações mais seletivas[39]. Como exemplo, pode-se citar as MNPs modificadas com grupamento C18 (Fe_3O_4@SiO_2-C18) no qual têm sido amplamente utilizadas na pré-concentração de matrizes ambientais[40,41]. Além disso, o uso de precursores híbridos de sílica com grupamentos reativos (Fe_3O_4@SiO_2-NH_2[42] Fe_3O_4@SiO_2-SH[43], Fe_3O_4@SiO_2-PITC[44], Fe_3O_4@SiO_2@γ-MPTS[45]) tem melhorado a interação sorbente-analito e estendido as possiblidades de modificação da superfície com outros materiais, tais como os polímeros impressos (Fe_3O_4@SiO_2-MIP) [46], grafeno e seus derivados (Fe_3O_4@SiO_2-G)[47] e líquidos iônicos (Fe_3O_4@SiO_2@ILs)[48]. A Figura 3 exemplifica um esquema de preparo e recobrimento das MNPs.

Recobrimentos baseados na tecnologia de polímeros impressos (polímeros molecularmente impressos (MIPs) e polímeros ionicamente impressos (IIPs)) apresentam como destaque a elevada seletividade por um analito devido a presença de cavidades seletivas. A estratégia de síntese não-covalente é a mais utilizada pois inúmeros precursores estão disponíveis e os analitos podem ser extraídos/eluídos sem envolver quebra de ligações químicas[50]. MIPs e IIPs podem ser baseados em polímeros inorgânicos, orgânicos ou híbridos. A grande vantagem dos materiais híbridos é a característica acumulada de ambos os polímeros.

Líquidos iônicos (ILs) são sais líquidos na temperatura de 25°C e apresentam excelentes propriedades de solvatação. Os ILs são altamente miscíveis e podem dissolver simultaneamente substâncias com características orgânicas e inorgânicas[51]. Nesse contexto, o recobrimento de MNPs com ILs tem sido desenvolvido com a vantagem de unir suas características químicas com a praticidade da MSPE[52]. No trabalho de Casado-Carmona et al.[53] foi feita a funcionalização dos grupos silanóis da sílica utilizando o IL MIM-PF_6, na superfície da MNP obtendo-se a Fe_3O_4@SiO_2@MIM-PF_6.

Óxido de grafeno (GO) é usualmente produzido através de forte oxidação do grafite, o método de obtenção amplamente utilizado é denominado de método de Hurmmers[54]. GO consiste de uma rede bidimensional baseada em anéis de carbono hexagonais que são covalentemente ligados com grupos funcionais de oxigênio (tais como hidroxila, epóxi e carboxila). Essa rede fornece boa solubilidade e dispersão desse material em muitos solventes, através da interação eletrostática e ligações de hidrogênio. Além disso, a estrutura bidimensional e a espessura conferem uma alta área superficial e capacidade de adsorção, portanto, a aplicação de GO em recobrimentos de MNPs é promissora[55,56]. Ding et al.[57] preparou MNPs de óxido de ferro recobertas com quitosana e modificadas com GO e ILs (Fe_3O_4@Quitosana-GO-FGILs). A elevada capacidade de extração do sorbentes pode ser atribuído a maior superfície de contato juntamente com maior interação entre a fase extratora e os analitos. Uma crescente vertente em novos recobrimentos para as MNPs está relacionada à redução do GO para o preparo de grafeno (G)[58].

Recobrimentos baseados em carbono podem apresentar elevada área superficial, baixa densidade, excelente flexibilidade e estabilidade química[59]. Na última década a preparação e aplicação de materiais

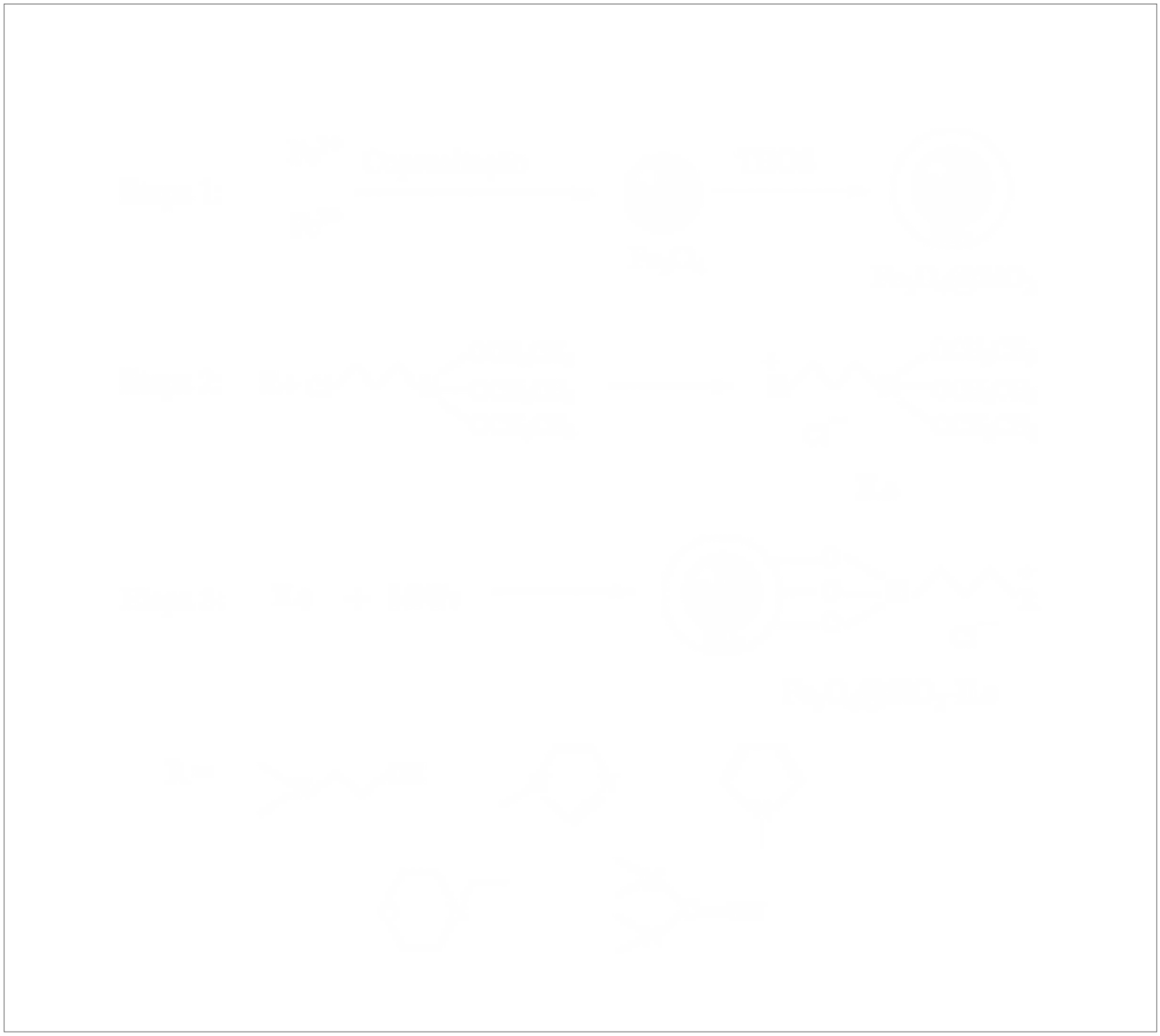

Figura 3. Esquema geral da síntese de MNPs de óxido de ferro recoberta com sílica e funcionalizada com líquido iônico (Fe_3O_4@SiO_2-ILs). Adaptado da ref (49) com permissão da Royal Society of Chemistry.

como nanotubos de carbono (CNTs) estão em evidência em química analítica[60]. Nessa vertente, Deng et al.[61] recobriu MNPs com nanotubos de carbono de paredes multiplas (MNPs/MWCNTs) para extração de pesticidas em amostras de chá.

Outra classe de materiais híbridos que recentemente tem se destacado no recobrimento de MNPs são as estruturas Metal-Orgânica (MOFs) as quais possuem interações através das ligações coordenadas. Entre as propriedades das MOFs, pode-se destacar a elevada área superficial, porosidade e tamanho dos poros uniformes, estabilidade térmica e possibilidade de outras funcionalizações a partir de sua superfície interna. Essas características associadas as MNPs podem criar sorbentes com uma capacidade extraordinária de adsorção[62].

Surfactantes e ácidos orgânicos com longas cadeias alquílicas também podem ser utilizados como um tipo de recobrimento para MNPs. Estes tipos de moléculas apresentam propriedades anfifílicas, isto é, conseguem interagir com partes polares (hidrofílicas) e apolares (hidrofóbicas). Nessa estratégia de recobrimento

ocorre a adsorção do surfactante na superfície do núcleo magnético formando admicelas e hemimicelas. Desta forma, são caracterizadas pela não formação de ligação química entre o núcleo magnético e o modificador. Nesta temática, três diferentes estratégias podem ser utilizadas para promover a adsorção do surfactante (dodecil sulfato de sódio, brometo de cetiltrimetil amônio, entre outros) no núcleo magnético[63,64].

No trabalho de Manafi et al.[65], NPs de Fe_3O_4@ SiO_2 foram funcionalizadas com etileno glicol bis-mercaptoacetato. A vantagem deste trabalho está relacionada a simplicidade e ao tempo reduzido para o recobrimento das MNPs. Além da boa capacidade de extração que pode ser atribuída as propriedades que os surfactantes apresentam (interações eletrostáticas hidrofílicas, π-cátion, e interações hidrofóbicas).

4. Aplicações da MSPE

A MSPE tem sido utilizada com a finalidade de extração, pré-concentração ou *clean up* de analitos orgânicos e inorgânicos. Uma das maiores vantagens desta técnica está relacionada a simplicidade operacional com boa eficiência de extração.

Os trabalhos utilizando a MSPE precisam ter seus parâmetros de extração otimizados (via processos univariados ou multivariados) para alcançar a máxima eficiência de extração. Entre os principais fatores, podemos destacar a quantidade de sorbente, tempo de extração, estratégia de agitação, pH da solução, efeito *salting out*, volume da amostra, tipo e quantidade de solvente de eluição[41,61].

Na Tabela 1 estão listados alguns trabalhos que usam a MSPE para a determinação de analitos em diferentes matrizes (ambiental, biológica, alimentos, entre outros) seguida pelas análises instrumentais (HPLC, GC, AAS, AES).

O trabalho de Abdolmohammad-Zadeh e Talleb[66] foi o primeiro a relatar a utilização de Fe_3O_4/ Mg-Al-nitrato LDH no procedimento de MSPE seguida pela detecção de quimioluminescência para separação, pré-concentração e determinação de quantidade ultra-traço de As(V) e As(III) em amostras de água. Essa metodologia apresentou vantagens como alta sorção cinética dos analitos e bons valores de precisão e exatidão.

Dimpe et al.[84] foi o primeiro a descrever a aplicação de AC@Fe_2O_3@MnO_2 na pré-concentração de metais refratários em amostras de águas por UA-d-MSPE/ICP-OES. A metodologia apresentou limite de detecção e quantificação na faixa de 0,0004-0,02 μg L^{-1} e 0,001-0,07 μg L^{-1}, respectivamente, e recuperação de 96-102%.

Diniz e Tarley[85] publicaram pela primeira vez a combinação da MSPE e extração em ponto nuvem (CPE) para pré-concentração de Cr(VI) e Cr(III) em amostras de águas por FAAS. O método baseou-se na utilização de Fe_3O_4@SiO_2-NH_2 obtendo LOD de 1,1 μg L^{-1} para Cr(VI) e 3,2 μg L^{-1} para Cr(III) e valores de recuperação na faixa de 91,4-103,5%. Bagheri et al.[71] foi o primeiro a publicar estruturas organometálicas [(Fe_3O_4–Piridina)/ $Cu_3(BTC)_2$] magnéticas com cavidades imobilizadas por Fe_3O_4-Piridina para extração e pré-concentração de Pd(II) em diferentes matrizes determinado por FAAS. Os parâmetros experimentais foram optimizados pela metodologia de Box-Behnken e os resultados apresentaram altos valores de pré-concentração, recuperação e boa seletividade do método

Ma et al.[45] trabalhou com amostras de água de lago, rio e cabelo humano. O intuito foi a quantificação de metil-mercúrio (CH_3Hg^+) e de mercúrio na forma inorgânica (Hg(II)) em razão dessas espécies serem potencialmente tóxicas. MNPs de Fe_3O_4@SiO_2@γ-MPTS foram aplicadas para as matrizes em estudo utilizando ICP-MS. Camba et al.[82] utilizou uma metodologia *in situ* de síntese das MNPs de Fe_3O_4 e extração de Cd(II) em amostras de água. Nesse método, o analito foi incorporado na estrutura rígida das MNPs com posterior análise por ETAAS pela decomposição das NPs e se apresentou ultrassensível para o Cd(II) com LOD de 2,3 ng L^{-1}.

Tabela 1. Aplicações de nanopartículas magnéticas em preparo de amostra.

Partícula magnética (quantidade, mg)	Analito extraído	Matriz (quantidade)	Técnica analítica	LOD	Rec. (%)	Ref.
Alimentos						
Fe_3O_4@SiO_2-MIPs (10,0 mg)	Ácido protocatecóico	Sucos de frutas (50 mL)	HPLC-UV	0,5 μg mL^{-1}	92 - 107	[67]
Fe_3O_4@TEOS-EGBMA (100 mg)	Aflatoxinas totais	Trigo (5 g)	FL	0,03 ng mL^{-1}	92 - 105	[65]
Fe_3O_4@SiO_2-C18 (60mg)	Pesticidas	Cenoura (200 mg)	GC-MS	0,0200 - 0,0392 ng g^{-1}	77 - 107	[68]
Fe_3O_4@poliestireno (50mg)	Piretróides	Vegetais (10 g)	HPLC-DAD	0,0200 - 0,0392 ng g^{-1}	91,6 - 116,2	[27]
Fe_3O_4@PDA (40 mg)	Corantes sintéticos	Pirulito (0,08 g); Bebidas em pó (0,1 g); Suco (16 g)	HPLC-DAD	0,20 - 0,25 μg L^{-1}	98,2 - 111,7	[69]
Fe_3O_4@TiO_2- 1-(2- piridilazo)-2-naftol (30 mg)	Aflatoxin M1	Leite (0,001 mL)	FAAS	13 ng L^{-1}	94,4 - 99,5	[70]
[(Fe_3O_4–Piridina)/$Cu_3(BTC)_2$] (30 mg)	Pb(II)	Peixe (0,5 g)	FAAS	0,37 ng mL^{-1}	102,6	[71]
Fe_3O_4@TiO_2-GO (0,5 g)	Hormônios	Leite (5 mL) Leite em pó (3 g)	HPLC-UV	4,3 – 7,5 ng mL^{-1}	70,6 - 94,5	[72]
Fe_3O_4@Murexida (14 mg)	Pb(II) e Cd(II)	Melão, maçã, uva e nectarina (0,5 g)	FAAS	Pb(II) = 1 μgL^{-1}; Cd(II) = 0,1 μgL^{-1}	Pb(II) = 98,2; Cd(II) = 97,5	[73]
Fe_3O_4@SiO_2 (5 mg)	Safranin T	Tomate e molho de tomate (1 g)	UHPLC-MS/MS	0,48 ng mL^{-1}	96,71 – 98,26	[74]
Fe_3O_4@SiO_2-IIP (10 mg)	Pb(II)	Músculo e fígado de boi, búfalo, alce, ovelha e bode (2 g)	FAAS	1,3 μg L^{-1}	98 - 115	[75]
Fe_3O_4@SiO_2@politiofeno (26 mg)	Hg(II)	Camarão, Atum enlatado e peixe (0,5 g)	CVAAS	0,02 ng mL^{-1}	102 - 109	[76]
Fe_3O_4@SiO_2-PITC (21 mg)	Cd(II) e Pb(II)	Peixe, camarão e atum enlatado (0,5 g)	FAAS	0,05 e 0,9 ng mL^{-1}	80-110	[44]
Ambiental						
Fe_3O_4@CTAB (55,5 mg)	4-nitrofenol e 4-clorofenol	Água (25 mL)	HPLC-DAD	0,05–0,1 μg L^{-1}	71,4–98,0	[77]
Fe_3O_4@SiO_2-C18 (30 mg)	microcistina-LR	Água (1000 mL)	HPLC-DAD	0,056 μg L^{-1}	73,3-104	[41]
Fe_3O_4@PDA/ZIF-7 (3 mg)	Hidrocarbonetos aromáticos policíclicos	Água de rio e amostras de ar (20 mL)	GC-MS	0,71–5,79 ng L^{-1}	>82	[78]
Fe_3O_4@SiO_2-GO	As(III) e As(V)	Água de nascente, rio, torneira e lago (70,0 mL)	ICP-MS	As(V) = 7,9 pg mL^{-1} As(V) = 28,0 pg mL^{-1}	72,55–109,71	[79]
Fe_3O_4@SiO_2–SH (60 mg)	CH_3Hg^+ e Hg(II)	Água de torneira, lago e mar (500 mL)	HPLC-ICP-MS	0,3 – 1,0 ng L^{-1}	96–104	[80]
Fe_3O_4@SiO_2-N-crisina (60 mg)	Cu(II)	Água de rio, lago e torneira (300 mL)	FAAS	0,3 ng mL-1	97-107	[81]
Fe_3O_4	Cd(II)	Água de poço, água pótavel, torneira e mineral	ETAAS	2,3 ng L^{-1}	98,2-100,3	[82]
Fe_3O_4@SiO_2 (50 mg)	Benzodiazepinas	Efluente (Água)	HPLC-DAD	0,021 – 0,065 μg mL^{-1}	90,5 - 98,6	[83]

Tabela 1. Aplicações de nanopartículas magnéticas em preparo de amostra.

Partícula magnética (quantidade, mg)	Analito extraído	Matriz (quantidade)	Técnica analítica	LOD	Rec. (%)	Ref.
Fe_3O_4@SiO_2-PITC (21 mg)	Cd(II) e Pb(II)	Água de torneira, oceano e rio; Solo (1 g)	FAAS	0,05 e 0,9 ng mL^{-1}	80 - 110	[44]
Fe_3O_4@ SiO_2-AAAPTS* (25 mg)	Bi(II) e Pb(II)	Água de torneira, água de poço	ETAAS	Bi(II) = 1,4 ng mL^{-1}; Pb(II) = 3,7ng mL^{-1}	Bi(II) = 101; Pb(II) = 101 - 103	[16]
Fe_3O_4@ SiO_2NH_2	Pb(II), Cu(II), Cd(II) e Hg(II)	Solução aquosa	Titulação de complexação	-	-	[42]
[(Fe_3O_4–Piridina)/$Cu_3(BTC)_2$] (30 mg)	Pb(II)	Sedimento (1 g) Água destilada, da torneira, mineral e de rio	FAAS	0.37 ng mL^{-1}	98,6 - 100,7	[71]
Fe_3O_4@Mg-Al-Nitrato LDH (150 mg)	As(V) e As(III)	Água de torneira, água de nascente, água de poço e água de chuva (200 mL)	CL	2 ng L^{-1}	As(V) = 100-106; As(III) = 100-104	[66]
Fe_3O_4@Murexida (14 mg)	Pb(II) e Cd(II)	Água da torneira e água do mar	FAAS	Pb(II) = 1 µg L^{-1} Cd(II) = 0,1 µg L^{-1}	Pb(II) = 98,2; Cd(II) = 97,5	[73]
AC@Fe_2O_3@MnO_2 (125 mg)	Ge, Hf, Mo, Nb, Sb, Ta, Te, Sn, Ti, W e Zr	Água de rio e água residual	ICP-OES	0,0004 - 0,02 µg L^{-1}	96-102	[84]
Fe_3O_4@SiO_2-amina (25 mg)	Cr(VI) e Cr(III)	Água da torneira, mineral e de lago	FAAS	Cr(VI) = 1,1 µg L^{-1} Cr(III) = 3,2 µg L^{-1}	91,4-103,5	[85]
Biológica						
Fe_3O_4@SiO_2@γ-MPTS (10 mg)	CH_3Hg^+ e Hg(II)	Cabelo	ICP-MS	1,6 - 1,9 ng L^{-1}	CH_3Hg^+ = 75,6 -99,6; Hg(II) = 81,3 -97,1	[45]
Fe_3O_4@SiO_2 (50 mg)	Benzodiazepinas	Cabelo (200 mg)	HPLC-DAD	0,0097 - 0,032 µg mL^{-1}	84,9 - 90,5	[83]
Fe_3O_4@SiO_2-MIPs (100 mg)	Paracetamol e tizanidine	Plasma Humano	UV-Vis	-	-	[86]
Fe_3O_4@UMS-C_{18} (50 mg)	Aminas aromáticas	Urina (20 mL)	UFLC-UV-Vis	1,3, 0,88, 1,1 e 1,1 ng mL^{-1}	70 - 125	[40]
Fe_3O_4@ SiO_2-AAAPTS* (25 mg)	Bi(II) e Pb(II)	Cabelo	ETAAS	Bi(II) = 1,4 ng mL^{-1}; Pb(II) = 3,7 ng mL^{-1}	Bi(II) e Pb(II) 100	[16]
Fe_3O_4@OA-IL* (100 mg)	Sulfonamida	Cabelo (200 mg)	HPLC-UV	1,2 - 1,9 ng g^{-1}	80	[87]
Outras matrizes						
Fe_3O_4@SiO_2@ILs (100 mg)	Bisphenol A	Utensílios plásticos (5 g)	HPLC - FLD-UV	90 ng·L^{-1}	99,6 - 100,4	[48]
Fe_3O_4-ANI*-NA* (7 mg)	Rodamina B	Espuma de lavar louça (1 g) detergente líquido (1 g), sombra de olhos (10 mg), xampu (1 g), lápis (10 mg), fósforo (10 mg)	FL	0,1 µg L^{-1}	94 - 99	[88]
Fe_3O_4@SiO_2-(p(4-VPBA-co-EGDMA) (100 mg)	Brassino-steróides	Tecidos de plantas (Brassica napus L.) (100 mg)	LC-MS-MS	0,27-1,29 pg mL^{-1}	93,0-97,4	[89]

Nos estudos de Ma et al.[41] foi reportado a funcionalização com C18 em uma MNPs recoberta com sílica, Fe_3O_4@SiO_2-C18, para a determinação de microcistina-LR em amostras de água para análise por HPLC-DAD. Com um tempo de extração de 15 minutos, o método apresentou LOD de 0,056 μg L^{-1} com recuperações de 73,3-104%.

Asgharinezhad e Ebrahimzadeh[77] desenvolveram MNPs de Fe_3O_4@CTAB para extrair 4-nitrofenol e 4-clorofenol de amostras de água seguida da análise por HPLC-DAD obtendo LOD de 0,05–0,1 μg L^{-1}. Mahpishanian e Sereshti[90] reportaram o uso de óxido de grafeno como sorbente para isolação e preconcentração da nicotina em amostras de água e obtiveram resultados promissores usando apenas 3 mg de fase extratora em 10 mL de amostra.

No estudo de Sheykhaghaei et al.[86], um processo simples e efetivo foi utilizado para o desenvolvimento de MNPs (Fe_3O_4@SiO_2-MIP) para determinação de paracetamol e tizanidina em plasma humano usando espectrofotometria de UV-vis. O método proposto obteve bons resultados para determinação de tizanidina, porém não apresentou seletividade para o paracetamol. Já Jiang et al.[40] sintetizou MNPs recobertas com sílica ultrafina funcionalizada com C18 (Fe_3O_4@UMS-C18) para a extração de quatro diferentes aminas aromáticas em amostras de urina por UFLC-UV obtendo-se LODs de 0,88 à 1,3 ng mL^{-1} e recuperações de 70-125%.

Yan et al.[87] preparou microesferas poliméricas magnéticas com líquido iônico modificado (Fe_3O_4@OA-ILs) para extração de compostos polares em urina. A alta percentagem de recuperação obtida (80 %) é resultado das interações π-π, dipolo-dipolo e atração eletrostática que ocorrem entre as sulfonamidas e o líquido iônico.

Zhang et al.[74] analisou safranina T, um tipo de corante sintético que pode ser prejudicial para seres humanos, em amostras de tomate, molho de tomate e yuba. Para isso, o autor utilizou duas técnicas de extração na sequência: primeiro usou-se a DLLME com ILs seguida pela MSPE com Fe_3O_4@SiO_2. O método proposto obteve recuperação na faixa de 96,71 à 98,26 % utilizando UHPLC-MS/MS.

Binellas e Stalikas[68] relatam o uso de MNPs Fe_3O_4@SiO_2-C18 para a extração de 26 agrotóxicos em amostras de cenoura usando CG-MS com LODs entre 1,0 - 46 μg kg^{-1}.

Xie et al.[67] desenvolveu MNPs com a tecnologia MIP (Fe_3O_4@SiO_2-MIP) para a extração seletiva de ácido protocatecóico em sucos por HPLC-UV. A extração magnética ocorreu rapidamente (10 s) com reutilização do sorbentes por seis vezes.

Manafi et al.[65] analisou o teor de aflatoxinas totais em amostras de trigo usando Fe_3O_4@TEOS-EGBMA. Além de ser constatado uma boa seletividade, as interações eletrostáticas com as micelas formadas pela adição de Triton X-100 aumentaram significativamente a sensibilidade do método analítico.

Abolhasani et al.[76] descreve em seu trabalho a aplicação de Fe_3O_4@SiO_2@politiofeno na pré-concentração e determinação de íons Hg(II) em frutos do mar. O planejamento experimental por Box-Behnken foi utilizado para investigar as condições apropriadas deste método através de sua superfície de resposta. Assim, Hg(II) foi determinado por CV-AAS obtendo um LOD de 0,02 ng mL^{-1}.

Uma abordagem diferente da aplicação das MNPs foi realizada por Tian et al.[72]. As MNPs (Fe_3O_4@TiO_2-GO) foram aprisionadas no interior de um chip microfluídico através da manipulação de campo magnético para a extração online de hormônios em amostras de leite e leite em pó.

5. Conclusões

O uso de NMPs em preparo de amostra é uma interessante estratégia, sob a perspectiva da química verde, para a quantificação de analitos em baixas concentrações na presença de potenciais interferentes. A MSPE é uma técnica simples e de rápida execução

devido a elevada área de contato do sorbente aliada a facilidade de separação das fases pela simples manipulação de um campo magnético externo. Adicionalmente, a possibilidade de reuso do material e a redução do consumo de solventes e sorbentes sem perda do desempenho analítico são algumas das características desta técnica que tem ganhado popularidade entre os pesquisadores.

Outrossim, podemos destacar a versatilidade em planejar sorbentes com características distintas pela simples alteração dos precursores (blocos construtores) dos recobrimentos. Atualmente, inúmeros precursores e modificadores estão disponíveis para melhorar a seletividade da extração pelo aumento da interação analito-sorbente.

Apesar do pequeno número de aplicações da MSPE no Brasil, as MNPs possuem um enorme potencial de crescimento nos próximos anos, principalmente no monitoramento de compostos orgânicos e inorgânicos em diversas matrizes complexas.

Agradecimentos

Os autores agradecem às agências de fomento Capes, CNPq e FUNDECT pelo apoio no desenvolvimento dos projetos de pesquisa.

Referências

[1] Fumes BH, Silva MR, Andrade FN, Nazario CED, Lanças FM. Recent advances and future trends in new materials for sample preparation. TrAC - Trends Anal Chem. 2015;71:9-25.

[2] Socas-Rodríguez B, Herrera-Herrera A V, Asensio-Ramos M, Hernández-Borges J. Dispersive Solid-Phase Extraction. In: Analytical Separation Science. Wiley-VCH; 2015. p. 1525–70.

[3] González-Sálamo J, Herrera-Herrera AV, Fanali C, Hernández-Borges J. Magnetic nanoparticles for solid-phase extraction. LC-GC Eur. 2016;29(4):180–93.

[4] Deng Y, Qi D, Deng C, Zhang X, Zhao D. Superparamagnetic High-Magnetization Microspheres with an Fe3O4@SiO2 Core and Perpendicularly Aligned Mesoporous SiO2 Shell for Removal of Microcystins. J Am Chem Soc. American Chemical Society; 2008 Jan 1;130(1):28–9.

[5] Towler PH, Smith JD, Dixon DR. Magnetic recovery of radium, lead and polonium from seawater samples after preconcentration on a magnetic adsorbent of manganese dioxide coated magnetite. Anal Chim Acta. 1996;328(1):53–9.

[6] Šafařík M, Šafařík I. Magnetic solid-phase extraction. J Magn Magn Mater. 1999;194(1):108–12.

[7] Francisquini E, Schoenmaker J, Souza JA. Nanopartículas magnéticas e suas aplicações. In p. 269–89.

[8] Dowling A, Clift R, Grobert N, Hutton D, Oliver R, O'neill O, et al. Nanoscience and nanotechnologies: opportunities and uncertainties. The Royal Society. 2004. 618-618 p.

[9] Beveridge JS, Stephens JR, Williams ME. The use of magnetic nanoparticles in analytical chemistry. Annu Rev Anal Chem. 2011;4:251–73.

[10] Rocío-Bautista P, Pino V. Extraction Methods Facilitated by the use of Magnetic Nanoparticles. In: Analytical Separation Science. Wiley-VCH; 2015. p. 1681–723.

[11] Cornell RM, Schwertmann U. 2nd ed. Wiley-VCH; 2003. 705 p.

[12] Wu W, Wu Z, Yu T, Jiang C, Kim W-S. Recent progress on magnetic iron oxide nanoparticles: synthesis, surface functional strategies and biomedical applications. Sci Technol Adv Mater. 2015;16(2):1–43.

[13] Knobel M, Nunes WC, Socolovsky LM, Biasi E De, Vargas JM, Denardin JC. Superparamagnetism and other magnetic features in granular materials: a review on ideal and real systems. J Nanosci Nanotechnol. 2008;8(4):2836–57.

[14] Wu W, He Q, Jiang C. Magnetic iron oxide nanoparticles: Synthesis and surface functionalization strategies. Nanoscale Res Lett. 2008;3(11):397–415.

[15] Tavengwa NT, Cukrowska E, Chimuka L. Synthesis, adsorption and selectivity studies of N-propyl quaternized magnetic poly(4-vinylpyridine) for hexavalent chromium. Talanta. 2013;116:670–7.

[16] Naghizadeh M, Taher MA, Behzadi M, Hassani Moghaddam F. Simultaneous preconcentration of bismuth and lead ions on modified magnetic core–shell nanoparticles and their determination by ETAAS. Chem Eng J. 2015;281:444–52.

[17] Shi H, Yang J, Zhu L, Yang Y, Yuan H, Yang Y, et al. Removal of Pb2+, Hg2+, and Cu2+by Chain-Like Fe3O4@SiO2@ Chitosan Magnetic Nanoparticles. J Nanosci Nanotechnol. 2016;16(2):1871–82.

[18] Pirbazari AE, Saberikhah E, Gorabi NGA. Fe3O4 nanoparticles loaded onto wheat straw: an efficient adsorbent for Basic Blue 9 adsorption from aqueous solution. Desalin Water Treat. 2014;1–12.

[19] Lai L, Xie Q, Chi L, Gu W, Wu D. Adsorption of phosphate from water by easily separable Fe3O4@SiO2 core/shell magnetic nanoparticles functionalized with hydrous lanthanum oxide. J Colloid Interface Sci. 2016;465:76–82.

[20] Rajput S, Pittman CU, Mohan D. Magnetic magnetite (Fe3O4) nanoparticle synthesis and applications for lead (Pb2+) and chromium (Cr6+) removal from water. J Colloid Interface Sci. 2016;468:334–46.

[21] Bao S, Tang L, Li K, Ning P, Peng J, Guo H, et al. Highly selective removal of Zn(II) ion from hot-dip galvanizing pickling waste with amino-functionalized Fe3O4@SiO2 magnetic nano-adsorbent. J Colloid Interface Sci. 2016;462:235–42.

[22] Teja AS, Koh P. Synthesis, properties, and applications of magnetic iron oxide nanoparticles. 2009;55:22–45.

[23] Zhang C, Yu Z, Zeng G, Huang B, Dong H, Huang J, et al. Phase transformation of crystalline iron oxides and their adsorption abilities for Pb and Cd. Chem Eng J 2016;284:247–59.

[24] Lu AH, Salabas EL, Schüth F. Magnetic nanoparticles: Synthesis, protection, functionalization, and application. Angew Chemie - Int Ed. 2007;46(8):1222–44.

[25] Jamshaid T, Neto ETT, Eissa MM, Zine N, Kunita MH, El-Salhi AE, et al. Magnetic particles: From preparation to lab-on-a-chip, biosensors, microsystems and microfluidics applications. TrAC - Trends Anal Chem. 2015;79:344–62.

[26] González-Sálamo J, Socas-Rodríguez B, Hernández-Borges J, Rodríguez-Delgado MÁ. Core-shell poly(dopamine) magnetic nanoparticles for the extraction of estrogenic mycotoxins from milk and yogurt prior to LC-MS analysis. Food Chem. 2017;215:362–8.

[27] Yu X, Yang H. Pyrethroid residue determination in organic and conventional vegetables using liquid-solid extraction coupled with magnetic solid phase extraction based on polystyrene-coated magnetic nanoparticles. Food Chem. 2016;217:303–10.

[28] Wang P, Wang X, Yu S, Zou Y, Wang J, Chen Z, et al. Silica coated Fe3O4 magnetic nanospheres for high removal of organic pollutants from wastewater. Chem Eng J. 2016;306:280–8.

[29] Philipse AP, Bruggen MPB Van, Pathmamanoharan C. Magnetic Silica Dispersions: Preparation and Stability of Surface-Modified Silica Particles with a Magnetic Core. Langmuir. 1994;10(17):92–9.

[30] Lu Y, Yin Y, Mayers BT, Xia Y. Modifying the Surface Properties of Superparamagnetic Iron Oxide Nanoparticles through a Sol-Gel Approach. Nano Lett. 2002;2(3):183–6.

[31] Andrade AL, Souza DM, Pereira MC, Fabris JD, Domingues RZ. Synthesis and characterization of magnetic nanoparticles coated with silica through a sol-gel approach. Ceramica. 2009;55:420–4.

[32] Im SH, Herricks T, Lee YT, Xia Y. Synthesis and characterization of monodisperse silica colloids loaded with superparamagnetic iron oxide nanoparticles. Chem Phys Lett. 2005;401(1–3):19–23.

[33] Deng YH, Wang CC, Hu JH, Yang WL, Fu SK. Investigation of formation of silica-coated magnetite nanoparticles via sol-gel approach. Colloids Surfaces A Physicochem Eng Asp. 2005;262(1–3):87–93.

[34] Zheng J, Yu Z, Ji G, Lin X, Lv H, Du Y. Reduction synthesis of FexOy@ SiO2 core – shell nanostructure with enhanced microwave-absorption properties. J Alloys Compd. 2014;602:8–15.

[35] Kobayashi Y, Horie M, Konno M, Rodriguez-Gonzalez B, Liz-Marzan LM. Preparation and properties of silica-coated cobalt nanoparticles. J Phys Chem B. 2003;107(30):7420–5.

[36] Tago T, Shibata Y, Hatsuta T, Miyajima K, Kishida M, Tashiro S, et al. Synthesis of silica-coated rhodium nanoparticles in reversed micellar solution. J Mater Sci. 2002;37(5):977–82.

[37] Dobson J, Tan W, Santra S, Tapec R, Theodoropoulou N, Dobson J. Synthesis and Characterization of Silica-Coated Iron Oxide Nanoparticles in Microemulsion: The Effect of Nonionic Surfactants Synthesis and Characterization of Silica-Coated Iron Oxide Nanoparticles in Microemulsion : The Effect of Nonionic. 2015;2900–6.

[38] Ding H, Zhang Y, Wang S, Xu J, Xu SC, Li G. Fe3O4@SiO2 core/shell nanoparticles: the silica coating regulations with a single-core for different core sizes and shell thicknesses. Chem M. 2012;24:4572–80.

[39] Sonmez M, Georgescu M, Alexandrescu L, Gurau D, Ficai A, Ficai D, et al. Synthesis and applications of Fe3O4/SiO2 core-shell materials. Curr Pharm Des. 2015;21(37):5324–35.

[40] Jiang C, Sun Y, Yu X, Gao Y, Zhang L, Wang Y, et al. Application of C18-functional magnetic nanoparticles for extraction of aromatic amines from human urine. J Chromatogr B Anal Technol Biomed Life Sci. 2014;947–948:49–56.

[41] Ma J, Yan F, Chen F, Jiang L, Li J, Chen L. C 18 -Functionalized Magnetic Silica Nanoparticles for Solid Phase Extraction of Microcystin-LR in Reservoir Water Samples Followed by HPLC-DAD Determination. J Liq Chromatogr Relat Technol. 2015;38(6):655–61.

[42] Mahmoud ME, Amira MF, Zaghloul AA, Ibrahim GAA. Microwave-enforced sorption of heavy metals from aqueous solutions on the surface of magnetic iron oxide-functionalized-3-aminopropyltriethoxysilane. Chem Eng J. 2016;293:200–6.

[43] Peng X, Zhang W, Gai L, Jiang H, Tian Y. Thiol-functionalized Fe3O4/SiO2 microspheres with superparamagnetism and their adsorption properties for Au(III) ion separation. Russ J Phys Chem A. 2016;90(8):1656–64.

[44] Tadjarodi A, Abbaszadeh A, Taghizadeh M, Shekari N, Asgharinezhad AA. Solid phase extraction of Cd(II) and Pb(II) ions based on a novel functionalized Fe3O4@ SiO2 core-shell nanoparticles with the aid of multivariate optimization methodology. Mater Sci Eng C. 2015;49:416–21.

[45] Ma S, He M, Chen B, Deng W, Zheng Q, Hu B. Magnetic solid phase extraction coupled with inductively coupled plasma mass spectrometry for the speciation of mercury in environmental water and human hair samples. Talanta. 2016;146:93–9.

[46] Hussain S, Khan S, Gul S, Pividori MI, Del Pilar Taboada Sotomayor M. A novel core@shell magnetic molecular imprinted nanoparticles for selective determination of folic acid in different food samples. React Funct Polym. 2016;106:51–6.

[47] Wang W, Ma R, Wu Q, Wang C, Wang Z. Magnetic microsphere-confined graphene for the extraction of polycyclic aromatic hydrocarbons from environmental water samples coupled with high performance liquid chromatography-fluorescence analysis. J Chromatogr A. 2013;1293:20–7.

[48] Chen S, Chen J, Zhu X. Solid phase extraction of bisphenol A using magnetic core-shell (Fe3O4@SiO2) nanoparticles coated with an ionic liquid, and its quantitation by HPLC. Microchim Acta. 2016;183(4):1315–21.

[49] Chen J, Wang Y, Ding X, Huang Y, Xu K. Magnetic solid-phase extraction of proteins based on hydroxy functional ionic liquid-modified magnetic nanoparticles. Anal Methods. 2014;6(20):8358–67.

[50] Martín-Esteban A. Molecularly-imprinted polymers as a versatile, highly selective tool in sample preparation. TrAC Trends Anal Chem. 2013;45:169–81.

[51] Marsh KN, Boxall JA, Lichtenthaler R. Room temperature ionic liquids and their mixtures - A review. Fluid Phase Equilib. 2004;219(1):93–8.

[52] Yue C, Fang D, Liu L, Yi TF. Synthesis and application of task-specific ionic liquids used as catalysts and/or solvents in organic unit reactions. J Mol Liq. 2011;163(3):99–121.

[53] Casado-Carmona FA, Alcudia-León M del C, Lucena R, Cárdenas S, Valcárcel M. Magnetic nanoparticles coated with ionic liquid for the extraction of endocrine disrupting compounds from waters. Microchem J. 2016;128:347–53.

[54] Hummers WS, Offeman RE. Preparation of Graphitic Oxide. J Am Chem Soc. 1958;80(6):1339–1339.

[55] Su S, Chen B, He M, Hu B, Xiao Z. Determination of trace/ultratrace rare earth elements in environmental samples by ICP-MS after magnetic solid phase extraction with Fe 3O4@SiO2@polyaniline-graphene oxide composite. Talanta. 2014;119:458–66.

[56] Wu L, Yu L, Ding X, Li P, Dai X, Chen X, et al. Magnetic solid-phase extraction based on graphene oxide for the determination of lignans in sesame oil. Food Chem. 2017;217.

[57] Ding X, Wang Y, Wang Y, Pan Q, Chen J, Huang Y, et al. Preparation of magnetic chitosan and graphene oxide-functional guanidinium ionic liquid composite for the solid-phase extraction of protein. Anal Chim Acta. 2015;861:36–46.

[58] Sha Y, Huang D, Zheng S, Deng C. Development of magnetic graphene as an adsorbent and matrix for selective enrichment and detection of crotonaldehyde in saliva by MALDI-TOF-MS. Anal Methods. 2013;5(18):4585–90.

[59] Gupta S, Tai N-H. Carbon materials as oil sorbents: a review on the synthesis and performance. J Mater Chem A. Royal Society of Chemistry; 2016;4(5):1550–65.

[60] Augusto F, Carasek E, Silva RGC, Rivellino SR, Batista AD, Martendal E. New sorbents for extraction and microextraction techniques. J Chromatogr A. 2010;1217(16):2533–42.

[61] Deng X, Guo Q, Chen X, Xue T, Wang H, Yao P. Rapid and effective sample clean-up based on magnetic multiwalled carbon nanotubes for the determination of pesticide residues in tea by gas chromatography-mass spectrometry. Food Chem. 2014;145:853–8.

[62] Tian J, Xu J, Zhu F, Lu T, Su C, Ouyang G. Application of nanomaterials in sample preparation. J Chromatogr A. 2013;1300:2–16.

[63] Pena-Pereira F, Duarte RMBO, Trindade T, Duarte AC. Determination of anionic surface active agents using silica coated magnetite nanoparticles modified with cationic surfactant aggregates. J Chromatogr A. 2013;1299:25–32.

[64] He H, Yuan D, Gao Z, Xiao D, He H, Dai H, et al. Mixed hemimicelles solid-phase extraction based on ionic liquid-coated Fe3O4/SiO2 nanoparticles for the determination of flavonoids in bio-matrix samples coupled with high performance liquid chromatography. J Chromatogr A. 2014;1324:78–85.

[65] Manafi MH, Allahyari M, Pourghazi K, Amoli-Diva M, Taherimaslak Z. Surfactant-enhanced spectrofluorimetric determination of total aflatoxins from wheat samples after magnetic solid-phase extraction using modified Fe3O4 nanoparticles. Spectrochim Acta - Part A Mol Biomol Spectrosc. 2015;146:43–9.

[66] Abdolmohammad-Zadeh H, Talleb Z. Speciation of As(III)/As(V) in water samples by a magnetic solid phase extraction based on Fe3O4/Mg-Al layered double hydroxide nano-hybrid followed by chemiluminescence detection. Talanta. 2014;128:147–55.

[67] Xie L, Guo J, Zhang Y, Shi S. Efficient determination of protocatechuic acid in fruit juices by selective and rapid magnetic molecular imprinted solid phase extraction coupled with HPLC. J Agric Food Chem. 2014;62(32):8221–8.

[68] Binellas CS, Stalikas CD. Magnetic octadecyl-based matrix solid-phase dispersion coupled with gas chromatography with mass spectrometry in a proof-of-concept determination of multi-class pesticide residues in carrots. J Sep Sci. 2015;38(20):3575–81.

[69] Chai W, Wang H, Zhang Y, Ding G. Preparation of polydopamine-coated magnetic nanoparticles for dispersive solid-phase extraction of water-soluble synthetic colorants in beverage samples with HPLC analysis. Talanta. 2016;149:13–20.

[70] Fasih Ramandi N, Shemirani F. Selective ionic liquid ferrofluid based dispersive-solid phase extraction for simultaneous preconcentration/separation of lead and cadmium in milk and biological samples. Talanta. 2015;131:404–11.

[71] Bagheri A, Taghizadeh M, Behbahani M, Akbar Asgharinezhad A, Salarian M, Dehghani A, et al. Synthesis and characterization of magnetic metal-organic framework (MOF) as a novel sorbent, and its optimization by experimental design methodology for determination of palladium in environmental samples. Talanta. 2012;99:132–9.

[72] Tian M, Feng W, Ye J, Jia Q. Preparation of Fe3O4@TiO2/graphene oxide magnetic microspheres for microchip-based preconcentration of estrogens in milk and milk powder samples. Anal Methods. 2013;5(16):3984.

[73] Asgharinezhad AA, Rezvani M, Ebrahimzadeh H, Shekari N, Ahmadinasab N, Loni M. Solid phase extraction of Cd(II) and Pb(II) ions based on a novel functionalized Fe3O4@ SiO2 core-shell nanoparticles with the aid of multivariate optimization methodology. Anal Methods. 2015;7:10350–8.

[74] Zhang L, Wu H, Liu Z, Gao N, Du L, Fu Y. Ionic Liquid-Magnetic Nanoparticle Microextraction of Safranin T in Food Samples. Food Anal Methods. 2015;8(3):541–8.

[75] Aboufazeli F, Zhad HRLZ, Sadeghi O, Karimi M, Najafi E. Novel ion imprinted polymer magnetic mesoporous silica nanoparticles for selective separation and determination of lead ions in food samples. Food Chem. 2013;141(4):3459–65.

[76] Abolhasani J, Hosseinzadeh Khanmiri R, Babazadeh M, Ghorbani-Kalhor E, Edjlali L, Hassanpour A. Determination of Hg(II) ions in sea food samples after extraction and preconcentration by novel Fe3O4@SiO2@polythiophene magnetic nanocomposite. Environ Monit Assess. 2015;187(9):554.

[77] Asgharinezhad AA, Ebrahimzadeh H. A simple and fast method based on mixed hemimicelles coated magnetite nanoparticles for simultaneous extraction of acidic and basic pollutants. Anal Bioanal Chem. 2016;408(2):473–86.

[78] Zhang S, Yao W, Ying J, Zhao H. Polydopamine-reinforced magnetization of zeolitic imidazolate framework ZIF-7 for magnetic solid-phase extraction of polycyclic aromatic hydrocarbons from the air-water environment. J Chromatogr A. 2016;1452:18–26.

[79] Rashidi Nodeh H, Wan Ibrahim WA, Ali I, Sanagi MM. Development of magnetic graphene oxide adsorbent for the removal and preconcentration of As(III) and As(V) species from environmental water samples. Environ Sci Pollut Res. 2016;23(10):9759–73.

[80] Zhang S, Luo H, Zhang Y, Li X, Liu J, Xu Q, et al. In situ rapid magnetic solid-phase extraction coupled with HPLC-ICP-MS for mercury speciation in environmental water. Microchem J. 2016;126:25–31.

[81] Abd Ali LI, Wan Ibrahim WA, Sulaiman A, Kamboh MA, Sanagi MM. New chrysin-functionalized silica-core shell magnetic nanoparticles for the magnetic solid phase extraction of copper ions from water samples. Talanta. 2016;148:191–9.

[82] Camba M, Romero V, Lavilla I, Bendicho C. In situ growth of Fe 3 O 4 nanoparticles for dispersive magnetic micro-solid phase extraction of cadmium followed by ETAAS detection. Anal Methods. 2015;7(3):1154–60.

[83] Esmaeili-Shahri E, Es'haghi Z. Superparamagnetic Fe3O4@SiO2 core-shell composite nanoparticles for the mixed hemimicelle solid-phase extraction of benzodiazepines from hair and wastewater samples before high-performance liquid chromatography analysis. J Sep Sci. 2015;38(23):4095–104.

[84] Dimpe KM, Nyaba L, Magoda C, Ngila JC, Nomngongo PN. Synthesis, modification, characterization and application of AC@ Fe2O3@MnO2 composite for ultrasound assisted dispersive solid phase microextraction of refractory metals in environmental samples. Chem Eng J. 2016;308:169–76.

[85] Diniz KM, Tarley CRT. Speciation analysis of chromium in water samples through sequential combination of dispersive magnetic solid phase extraction using mesoporous amino-functionalized Fe3O4/SiO2 nanoparticles and cloud point extraction. Microchem J. 2015;123:185–95.

[86] Sheykhaghaei G, Hosaini M, Khanahmadzadeh S. Synthesis and characterization of the core-shell magnetic molecularly imprinted polymer nanoparticles for selective extraction of tizanidine in human plasma. Bull Mater Sci. 2016;39(3):647–53.

[87] Yan H, Gao M, Yang C, Qiu M. Ionic liquid-modified magnetic polymeric microspheres as dispersive solid phase extraction adsorbent: A separation strategy applied to the screening of sulfamonomethoxine and sulfachloropyrazine from urine. Anal Bioanal Chem. 2014;406(11):2669–77.

[88] Bagheri H, Daliri R, Roostaie A. A novel magnetic poly(aniline-naphthylamine)-based nanocomposite for micro solid phase extraction of rhodamine B. Anal Chim Acta. 2013;794:38–46.

[89] Ding J, Mao LJ, Guo N, Yu L, Feng YQ. Determination of endogenous brassinosteroids using sequential magnetic solid phase extraction followed by in situ derivatization/desorption method coupled with liquid chromatography-tandem mass spectrometry. J Chromatogr A. 2016;1446:103–13.

[90] Mahpishanian S, Sereshti H. Graphene oxide-based dispersive micro-solid phase extraction for separation and preconcentration of nicotine from biological and environmental water samples followed by gas chromatography-flame ionization detection. Talanta 2014;130:71–7.

Símbolos e abreviaturas

Acac - Acetitacetonato

AOT - Bis (2-etil-hexil) sulfosuccinato de sódio

CNTs - Nanotubos de carbono

CTAB - Brometo de cetiltrimetilamônio

Cup - N-nitrofenilhidroxiamina

G - Grafeno

GO - Oxido de grafeno

IIP – Polímeros ionicamente impresso

IL - Líquido iônico

LDH - Dupla camada de hidróxido

MIM - Hexafluorofosfato de metilimidazólio

MIP - Polímeros molecularmente impresso

MNP - Nanopartícula magnética

MOFs - Estruturas Metal-Orgânica

MWCNTs - Nanotubos de carbono de paredes multiplas

Nps - Nanopartículas

Journal of Chromatography B, 947–948 (2014) 49–56

Contents lists available at ScienceDirect

Journal of Chromatography B

journal homepage: www.elsevier.com/locate/chromb

Application of C_{18}-functional magnetic nanoparticles for extraction of aromatic amines from human urine

Chunzhu Jiang, Ying Sun, Xi Yu, Yan Gao, Lei Zhang, Yuanpeng Wang, Hanqi Zhang, Daqian Song*

College of Chemistry, Jilin University, Qianjin Street 2699, Changchun 130012, PR China

ARTICLE INFO

Article history:
Received 26 August 2012
Received in revised form 21 August 2013
Accepted 2 December 2013
Available online 17 December 2013

Keywords:
Human urine
Aromatic amines
C_{18}-functional ultrafine magnetic silica nanoparticles
Magnetic solid-phase extraction
Ultra fast liquid chromatography

ABSTRACT

In this paper, a novel method using C_{18}-functional ultrafine magnetic silica nanoparticles (C_{18}-UMS NPs) as adsorbents was developed for rapid extraction and enrichment of aromatic amines from urine. C_{18}-UMS NPs were prepared by chemical coprecipitation, silanization and alkylation. The aromatic amines can be adsorbed on C_{18}-UMS NPs and isolated easily from the matrix with an external magnetic field. After desorption with acetonitrile, the aromatic amines were determined by ultra fast liquid chromatography. The experimental parameters, such as pH value of sample solution, amount of C_{18}-UMS NPs, extraction time, type and volume of desorption solvent, and desorption time were optimized. The analytical performances of the present method were also evaluated. The limits of detection for 1-aminonaphthalene, 4-aminobiphenyl, 4,4′-diaminodiphenylmethane and 4-aminophenylthioether were 1.3, 0.88, 1.1 and 1.1 ng mL^{-1}, respectively. The results showed that the present method was simple, highly efficient and rapid for the extraction and enrichment of aromatic amines from urine.

1. Introduction

There are various kinds of aromatic amines in the surrounding living environments, such as, aniline, benzidine, 4-aminophenylthiother, *p*-chloroaniline and so on [1,2]. They are toxic and carcinogenic. The concentration of aniline in drinking water is limited to 100 ng mL^{-1} [3]. Aromatic amines are widely used as raw materials or intermediates in the manufacturing of industrial chemicals such as pesticides, pharmaceuticals, explosives, rubber, epoxy polymers, cosmetics, dye stuff plants and aromatic polyurethanes [4–6]. The concentration of these amines in textile and leather articles is limited to 30 μg g^{-1} by European Union regulations [7]. In some other countries, the acceptable limits were lower, e.g., 20 μg g^{-1} in textiles [8]. The uses of carcinogenic aromatic amines have caused great harm to human health [9]. Carcinogenic aromatic amines were detectable in several commercial hair dyes [10]. The known bladder carcinogen 4-aminobiphenyl (4-ABP) was detectable in several commercial hair dyes in levels up to 12.8 ng mL^{-1} [11]. The use of aromatic amines can increase the risk of cancer because they can be easily absorbed through the skin. These aromatic amines, such as 4-ABP, are important carcinogenic agents in tobacco smoke [12]. Environmental tobacco smoke should be a source of aromatic amines. When the azo dyes were absorbed by oral ingestion (particularly by babies sucking on toys and textiles containing these dyes) and through sweat or via frication with clothing, the azo dyes can be degraded to release aromatic amines in liver cells, extrahepatic tissue and epidermal cells [7]. The carcinogenic aromatic amines in the body can harm human health. The determination of aromatic amines in human urine is particularly important.

Wu et al. extracted and separated aromatic amines in lake water by solid phase microextraction (SPME) [13]. Dasgupta extracted aromatic amines by liquid-liquid extraction (LLE) [14]. However, the methods in these studies are time-consuming and organic solvent wasting. So it is necessary to develop a simple, rapid and reliable sample pretreatment method for the determination of aromatic amines.

Recently, magnetic nanoparticles (MNPs) have received increasing attention. Generally, MNPs are prepared by encapsulating inorganic magnetic cores (mainly Fe_3O_4 core) with organic polymer or inorganics [15,16]. Because of their large surface areas, unique physical and chemical properties, the MNPs have been widely used in many fields, such as biotechnology, biomedicine, protein separation, removal of metal ions and dyes [17–21]. The paramagnetic properties of these particles allow the easy isolation of products from solution by the external magnetic field. Thus, suspended MNPs tagged with analytes can be isolated from large volume samples using a magnet. The isolation and purification of the MNPs are easier and faster than those of other materials. In recent years, the MNPs were widely

* Corresponding author. Tel.: +86 0431 85168399; fax: +86 0431 85112355.
E-mail address: songdq@jlu.edu.cn (D. Song).

1570-0232/$ – see front matter © 2013 Elsevier B.V. All rights reserved.
http://dx.doi.org/10.1016/j.jchromb.2013.12.008

used in analytical chemistry. Parham et al. utilized magnetic iron oxide nanoparticles to extract fluoride in water samples [22]. Zhao et al. synthesized silica–magnetite nanoparticle mixed hemimicelle sorbents for rapid extraction of typical phenolic compounds from environmental water samples [23]. Gao et al. prepared magnetite–silica–poly(methacrylic acid-*co*-ethylene glycol dimethacrylate) sorbents and investigated the efficiency of these nanoparticles in extraction of sulfonamide in milk samples [24].

To the best of our knowledge, few papers have been reported on the use of MNPs to extract and preconcentrate analytes in human urine. In this study, C_{18}-functional ultrafine magnetic silica nanoparticles (C_{18}-UMS NPs) were synthesized by coating ultrafine Fe_3O_4 NPs with silica and subsequently immobilizing dimethyl octadecyl chlorosilane (OCS) on the nanoparticles. These MNPs were used for the extraction of aromatic amines in human urine based on magnetic solid-phase extraction (MSPE). Due to the high surface area and the excellent adsorption capacity of these MNPs, satisfactory extraction recoveries of aromatic amines could be achieved. The aromatic amines were analyzed by the ultra fast liquid chromatography (UFLC). C_{18}-UMS NPs show high performance potential in processing complicated samples.

2. Experimental

2.1. Chemicals

The standards of 1-aminonaphthalene (AN, *p*Ka, 3.92, log *P*, 3.2), 4-aminobiphenyl (4-ABP, *p*Ka, 4.35, log *P*, 2.9), 4,4′-diaminodiphenylmethane (4,4′-DADP, *p*Ka, 4.96, log *P*, 1.6) and 4-aminophenylthioether (4-APT) were obtained from J&K Scientific (Fig. S1). Appropriate amounts of the compounds were dissolved in methanol to prepare 500 μg mL^{-1} stock standard solutions of each compound. Then the mixed stock solution containing all compounds (10 μg mL^{-1}) was prepared from individual stock standard solution by diluting with methanol and stored under dark condition at 4 °C. Dimethyl octadecyl chlorosilane (OCS) was supplied by Alfa Aesar (USA). Iron(II) chloride tetrahydrate ($FeCl_2{\cdot}4H_2O$), iron(III) chloride hexahydrate ($FeCl_3{\cdot}6H_2O$) and sodium hydroxide were supplied by Guangfu Fine Chemical Research Institute (Tianjin, China). Chromatographic-grade methanol and acetonitrile were purchased from Fisher (New Jersey, USA). Analytical-grade toluene, triethylamine, *n*-hexane, ethanol, isopropanol, tetraethyl orthosilicate (TEOS), ammonia, hydrochloric acid were obtained from Beijing Chemical Works (Beijing, China). The deionized water was prepared with Milli-Q water purification system (Millipore, Bedford, MA, USA).

2.2. Preparation of C_{18}-functionalized ultrafine magnetic silica nanoparticles

The magnetic nanoparticles, C_{18}-functionalized ultrafine magnetic silica nanoparticles (C_{18}-UMS NPs), were synthesized by chemical coprecipitation, silanization and alkylation method. First, $FeCl_2{\cdot}4H_2O$ (1.0 g), $FeCl_3{\cdot}6H_2O$ (2.6 g) and HCl (12 mol L^{-1}, 0.425 mL) were added in 12.5 mL of deionized water. The mixture was added dropwise into 125 mL NaOH solution (1.5 mol L^{-1}) under vigorous stirring with nitrogen gas passing continuously through the solution. The reactor was placed into an 80 °C water bath and the mixture was stirred vigorously for 3 h. The obtained Fe_3O_4 NPs precipitate was separated from the reaction medium under the magnetic field and washed with 100 mL deionized water four times. The amount of Fe_3O_4 NPs was 1.0 g and the yield is 90.05% (in Fe content). Then, the newly prepared Fe_3O_4 NPs were added into a solution containing deionized water (6 mL), isopropanol (43 mL) and 1.25 mL of ammonia (25%, m/m). After stirring for 15 min with nitrogen gas passing through the solution, TEOS (125 μL) was added into the solution. The resulting solution was then allowed to stand for 4 h at room temperature under continuous stirring. Then the magnetic silica nanoparticles were washed with deionized water three times and dried in a vacuum oven at 60 °C. The dried magnetic silica microspheres (0.6 g) were added into 30 mL of anhydrous toluene. The resulting mixture was heated to boiling, and then 0.6 mL of triethylamine and 0.9 g of OCS were added in the mixture. The mixture was then refluxed for 5 h. The obtained C_{18}-UMS NPs were washed and dried (Fig. S2a).

2.3. MSPE procedure

Firstly, 20 mL of filtered urine sample was adjusted to pH 9 by adding 2 mL of pH 9 phosphate buffer. 50 mg of C_{18}-UMS NPs was added into the urine sample. The mixture was stirred for 20 min. Subsequently, C_{18}-UMS NPs adsorbing aromatic amines were isolated with a strong magnet at the bottom of the container and the supernatant was poured out. The C_{18}-UMS NPs were washed with 1 mL of deionized water. C_{18}-UMS NPs adsorbing aromatic amines were placed in 3 mL of acetonitrile, and the resulting mixture was stirred for 1 min. The aromatic amines were eluted into acetonitrile. After the C_{18}-UMS NPs were removed, the eluate was dried under a stream of nitrogen at 50 °C and the residue was dissolved in 0.2 mL of methanol. 3 μL of this solution was injected into the UFLC system for analysis. When the mixture of methanol–water was used to dissolve the residue, the peaks shapes of aromatic amines were slightly better than those obtained with the methanol and the recoveries of aromatic amines slightly decreased. Finally, methanol was used to dissolve the residue (Fig. S2b). C_{18}-UMS NPs can be recycled by washing with methanol for 8 min, deionized water for 8 min and methanol for 10 min.

2.4. UFLC determination

The aromatic amines were separated and determined using an ultra fast liquid chromatographic (UFLC) system (Shimadzu Corporation, Kyoto, Japan) equipped with two LC-20AD pumps, a SIL-20A automatic sample injector, a CTO-20A column oven and a SPD-20A UV–vis detector. The separation was performed on a Shimadzu XR-ODS column (75 mm × 2 mm, 2.2 μm particle size). The mobile phase was the mixture of methanol and water (50:50, v/v) and the flow-rate was set at 0.2 mL min^{-1}. The monitoring wavelength was 240 nm for AN, 4,4′-DADP and 280 nm for 4-ABP, 4-APT. The temperature of column was controlled at 30 °C. Injection volume was 3 μL.

2.5. Human urine samples

The present method was applied to the analysis of urine samples from three donors (sample 1, sample 2, and sample 3) who are working in education and other two donors (sample 4 and sample 5) who are working in tobacco company. The mean age of urine human donors is 36.2.The samples were taken and immediately collected in sterilized 500 mL of polyethylene bottles. All urine samples were filtered through 0.45 μm nylon membranes (Shanghai Institute of Pharmaceutical Industry, China) and analyzed directly in triplicate. The spiked urine samples were prepared by adding standard solution of aromatic amines into the real urine samples.

3. Results and discussion

3.1. Characterization of C_{18}-UMS NPs

The synthesis of C_{18}-UMS NPs involves three steps: chemical coprecipitation, silanization and alkylation. Observation by

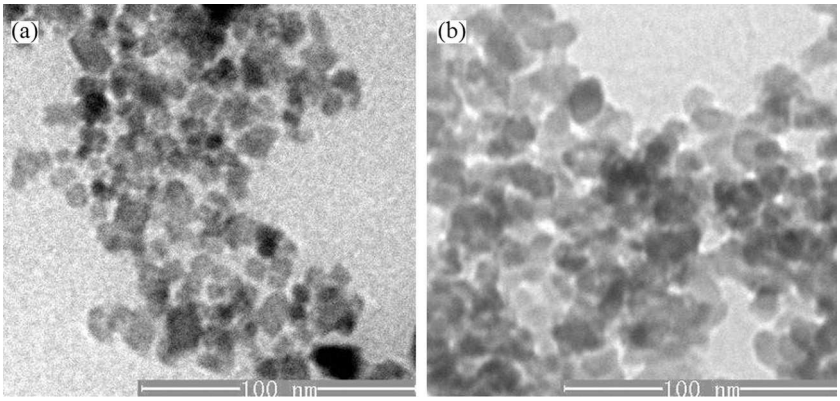

Fig. 1. TEM images of (a) Fe_3O_4 NPs and (b) C_{18}-UMS NPs.

transmission electron microscopy (TEM) shows uniform size distribution of the Fe_3O_4 NPs and C_{18}-UMS NPs (Fig. 1). The Fe_3O_4 NPs are 8–10 nm in diameter, and C_{18}-UMS NPs are 13–15 nm in diameter. Magnetic characterization was carried out by magnetometry at 300 K using a superconducting quantum interference device (SQUID). As shown in Fig. 2, there is no hysteresis, remanence and coercivity, suggesting that Fe_3O_4 NPs, Fe_3O_4–SiO_2 NPs, and C_{18}-UMS NPs are typically superparamagnetic. The saturation intensities of magnetization are 58.45 emu g^{-1} for Fe_3O_4 NPs, 55.42 emu g^{-1} for Fe_3O_4–SiO_2 NPs, and 40.12 emu g^{-1} for C_{18}-UMS NPs. Apparently, the nonmagnetic SiO_2 and C_{18} coating on the Fe_3O_4 NPs result in the decrease of the magnetic strength for C_{18}-UMS NPs. The magnetic saturation value of C_{18}-UMS NPs is still sufficient for rapid magnetic separation with a conventional magnet. FT-IR spectroscopy was applied to characterize the Fe_3O_4–SiO_2 NPs and these nanoparticles after modification with OCS. The absorption peak at 580 cm^{-1} is attributed to Fe–O–Fe vibration of magnetite (Fig. 3a). The absorbing peak of 1110–1000 cm^{-1} is attributed to the Si–O–Si stretching vibration of silica layer formed on the surface of magnetite nanoparticles. The absorption peak at ~1640 cm^{-1} can be assigned to the adsorbed water on the silica shell or the silanol groups of the silica. After surface modification, the new absorption peak at ~2960 cm^{-1} is ascribed to CH_2 originated from silane coupling agent, suggesting that the alkyl groups have been successfully grafted on the surface of magnetic silica microspheres (Fig. 3b).

3.2. Optimization of the MSPE conditions

3.2.1. Effect of pH values of urine samples

An appropriate pH value is beneficial to improvement of the adsorption efficiency and elimination of interference. Therefore, it is necessary to adjust the pH value of urine sample prior to MSPE in order to detain high enrichment factor. The effect of pH values was examined in the range of 5–11 when the other conditions were unchanged. Fig. 4 demonstrates the effect of pH on the recoveries of aromatic amines. Different analytes show different trend with the increase of pH values. As shown in Fig. 4, the recoveries of 4, 4′-DADP and 4-APT increase with the increase of the pH value and the highest recoveries of these analytes are obtained when the pH value is 9. While the recoveries of AN and 4-ABP decrease with the increase of the pH value in the range of 5–8 and then increase with the increase of the pH value in the range of 8–11. The recoveries of AN and 4-ABP do not increase significantly when the pH values is higher than 9. Finally pH 9 is selected for next experiments.

3.2.2. Effect of the amount of C_{18}-UMS NPs

The mechanism of extraction of aromatic amines with these C_{18}-UMS NPs was based on the distribution of analytes between the different phases. Because of the different chemical structures of the four kinds of analytes, the recoveries are also slightly different. The recoveries of analytes which contain chain group similar to C_{18} are slightly higher.

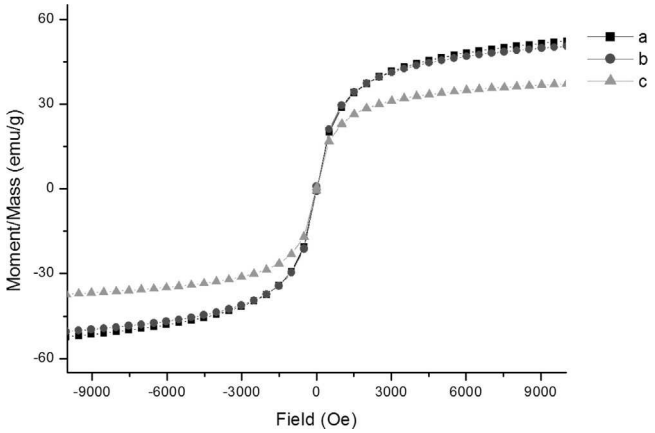

Fig. 2. Room-temperature magnetization curves of (a) Fe_3O_4 NPs, (b) Fe_3O_4–SiO_2 NPs, and (c) C_{18}-UMS NPs.

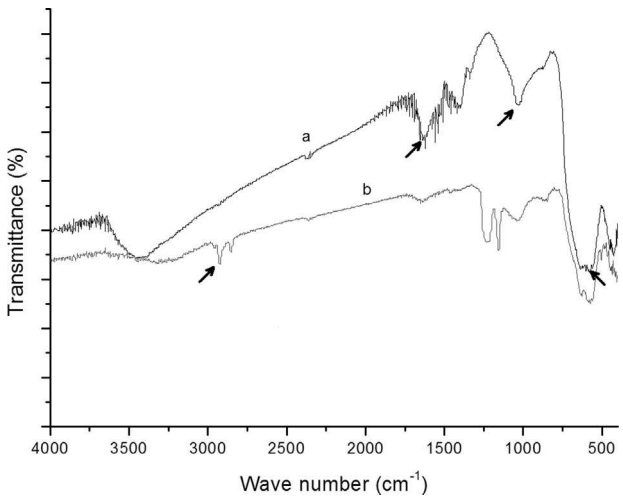

Fig. 3. FT-IR spectra of (a) Fe_3O_4–SiO_2 NPs and (b) C_{18}-UMS NPs.

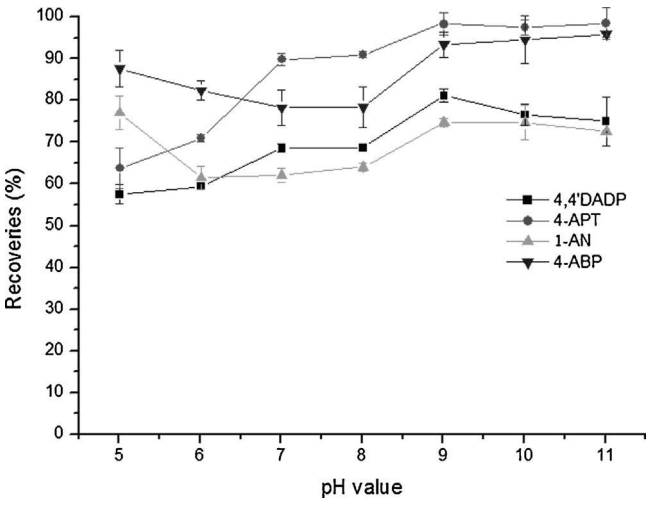

Fig. 4. Effect of pH values of sample solution on recoveries of aromatic amines. C_{18}-UMS NPs, 50 mg; extraction time, 25 min; desorption solvent, methanol; volume of desorption solvent, 4 mL; desorption time, 3 min.

The effect of amount of the C_{18}-UMS NPs was investigated (Fig. S3). The recoveries of aromatic amines increase with the increase of the amount of C_{18}-UMS NPs. When the amount of adsorbents is larger than 40 mg, the recoveries of the aromatic amines reach the maximum. According to the above results, 50 mg of C_{18}-UMS NPs is selected as the amount of magnetic adsorbents used for extraction of aromatic amines in this experimental.

3.2.3. Effect of the extraction time

In the MSPE, the extraction time is one of the prime factors. The effect of extraction time was examined. From Fig. 5, we can find that the recoveries of aromatic amines increase with the increase of the extraction time. The highest recoveries of aromatic amines are obtained when extraction time is 20 min. However, the recoveries do not increase when the extraction time increase from 20 to 35 min. Therefore, 20 min was selected as the extraction time of the aromatic amines in urine samples.

Meanwhile, C_{18}-functional ultrafine magnetic silica nanoparticles possessed superparamagnetism and large saturation magnetization which enabled them to be completely isolated in a short time (shorter than 2 min) with a strong magnet. In a word, because of rapid separation rate the analytical time was significantly shortened.

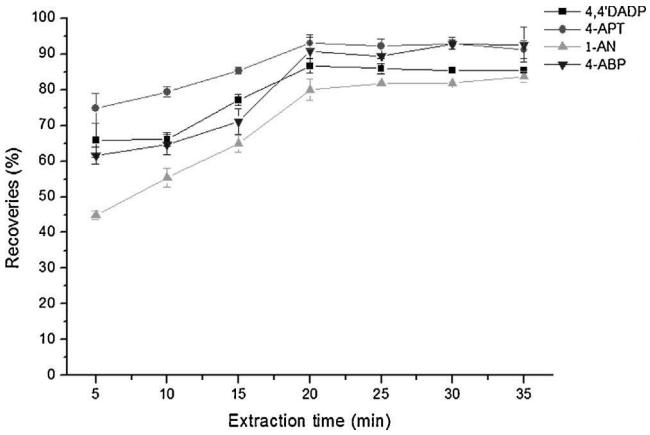

Fig. 5. Effect of the extraction time on recoveries of aromatic amines. The pH value, 9; C_{18}-UMS NPs, 50 mg; desorption solvent, methanol; volume of desorption solvent, 4 mL; desorption time, 3 min.

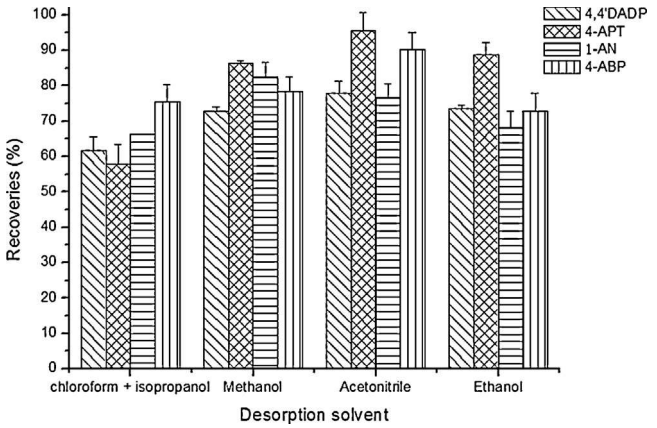

Fig. 6. Effect of the desorption solvent on recoveries of aromatic amines. The pH value, 9; C_{18}-UMS NPs, 50 mg; extraction time, 20 min; volume of desorption solvent, 4 mL; desorption time, 3 min.

3.2.4. Effect of the desorption solvent

The mechanism of desortion of aromatic amines from NPs was based on the distribution of analytes between the different phases. In order to obtain the high recoveries of aromatic amines, four kinds of organic solvents, including chloroform isopropanol mixture (10:90, v/v), methanol, acetonitrile and ethanol were used as desorption solvent and the results are shown in Fig. 6. From Fig. 6, we can find that all the four desorption solvents can desorb AN and 4,4′-DADP from C_{18}-UMS NPs effectively. To desorb 4-ABP and 4-APT, the desorption capacity of acetonitrile was significantly greater than these of the other three solvents. Therefore, acetonitrile is used as the desorption solvent.

3.2.5. Effect of the volume of desorption solvent

The volume of desorption solvent was also investigated (Fig. S4). The increase of the volume of desorption solvent do not affect the recoveries of 4,4′-DADP and 4-APT significantly. However, when the volume of desorption solvent is 3 mL, the recoveries of AN and 4-ABP are higher than those obtained with the other volumes of desorption solvent. Therefore, 3 mL is selected as the volume of acetonitrile which is valid for the amount of NPs used and the quantity of aromatic amines contained in the tested sample.

3.2.6. Effect of the desorption time

The effect of desorption times (0.5, 1, 2, 3, 4 and 5 min) was investigated (Fig. S5). With the increase of desorption time, the recoveries of aromatic amines do not change significantly. Finally, 1 min was selected as the desorption time.

3.3. Reusability of the magnetic adsorbents

In order to investigate the effectiveness of the nanoparticle adsorbents, the C_{18}-UMS NPs were reused in MSPE (Fig. S6). The C_{18}-UMS NPs were recycled by washing with methanol for 8 min, deionized water for 8 min and methanol for 10 min before the reuse. The experimental results indicate that the recoveries of analytes decrease only slightly when the adsorbents are reused 8 times.

3.4. Analytical performance

When the mixed standard solution is directly injected into the UFLC, the limits of detection (LODs) of 4,4′-DADP, 4-APT, AN and 4-ABP are 66.5, 94.4, 45.9 and 39.6 ng mL^{-1}, respectively. The limits of quantification (LOQs) of the analytes are 221.8, 314.6, 153.0 and 132.1 ng mL^{-1}, respectively. The chromatograms of the standard solution are shown in Fig. 7.

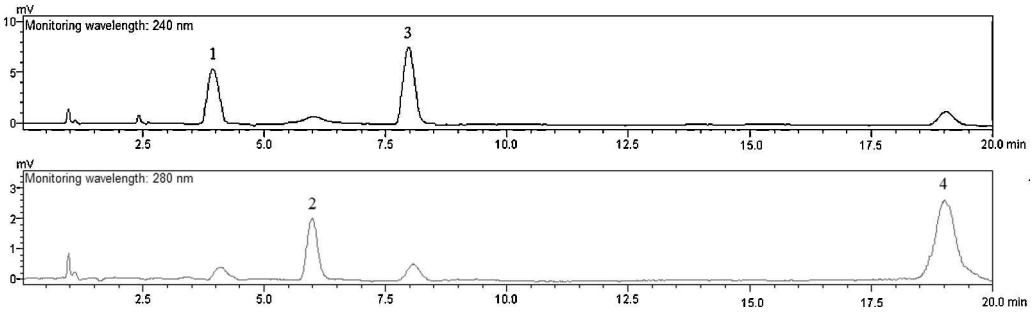

Fig. 7. The chromatograms of the standard solution. (1) 4,4′-DADP; (2) 4-APT; (3) AN; and (4) 4-ABP.

Table 1
Calibration equations, LODs and LOQs for total aromatic amines.

Analyte	Linear range (ng mL^{-1})	Calibration equations	Correlation coefficient (r)	LOD (ng mL^{-1})	LOQ (ng mL^{-1})
4, 4′-DADP	5–500	$y = 10{,}000 + 1591.4x$	0.9998	1.1	3.5
4-APT	5–500	$y = -1297.2 + 1220.7x$	0.9992	1.1	3.6
AN	5–500	$y = 14634 + 1353.4x$	0.9997	1.3	4.3
4-ABP	5–500	$y = 2971.5 + 2179.7x$	0.9998	0.88	2.9

Table 2
The intra- and inter-day precision and recoveries ($n = 6$).

Analyte	Concentration (ng mL^{-1})	Intra-day precision		Inter-day precision	
		Recovery (%)	RSD (%)	Recovery (%)	RSD (%)
4,4′-DADP	10.0	94.5	2.7	88.8	6.9
	20.0	99.0	2.1	89.8	5.3
	250.0	100.1	0.6	98.4	3.7
4-APT	10.0	96.2	2.5	100.8	4.9
	20.0	95.5	7.0	88.7	4.1
	250.0	92.7	6.2	102.8	2.9
AN	10.0	94.5	7.9	95.4	7.8
	20.0	102.7	3.3	90.4	10.0
	250.0	100.5	2.9	94.7	4.2
4-ABP	10.0	105.4	6.4	98.4	5.4
	20.0	91.7	1.5	96.9	2.4
	250.0	101.4	1.7	99.7	3.1

Table 3
Analytical results of urine samples ($n = 3$).

Urine sample	Added (ng ml^{-1})	4,4′-DADP		4-APT		AN		4-ABP	
		Found (ng mL^{-1})	Recovery (%)	Found (ng mL^{-1})	Recovery (%)	Found (ng mL^{-1})	Recovery (%)	Found (ng mL^{-1})	Recovery (%)
Sample 1	0.0	0.0		0.0		0.0		0.0	
	10.0	9.2	92.1 ± 2.8	8.8	87.7 ± 3.1	9.9	98.6 ± 2.8	9.8	98.0 ± 1.6
	20.0	18.0	90.4 ± 5.3	17.5	87.7 ± 4.3	16.9	84.4 ± 5.6	19.2	95.8 ± 4.7
	200.0	187.2	93.6 ± 4.2	192.8	96.4 ± 2.9	174.5	87.3 ± 4.5	193.5	96.8 ± 4.1
Sample 2	0.0	0.0		0.0		0.0		0.0	
	10.0	9.4	94.2 ± 2.6	9.1	91.0 ± 4.3	8.2	82.1 ± 5.7	9.0	90.4 ± 3.0
	20.0	18.8	93.8 ± 0.9	18.9	94.6 ± 2.2	16.00	79.8 ± 1.7	16.8	83.9 ± 4.6
	200.0	183.6	91.8 ± 3.5	194.8	97.4 ± 3.7	170.7	85.3 ± 7.1	198.1	99.1 ± 3.3
Sample 3	0.0	0.0		0.0		0.0		0.0	
	10.0	8.7	87.3 ± 2.0	8.9	89.1 ± 1.5	7.8	78.5 ± 2.9	7.8	78.4 ± 2.4
	20.0	16.2	81.2 ± 1.7	15.6	77.8 ± 0.7	14.1	70.7 ± 3.6	16.6	83.0 ± 3.2
	200.0	158.5	79.3 ± 3.1	162.6	81.3 ± 6.2	167.3	83.6 ± 4.8	159.5	79.7 ± 2.8
Sample 4	0.0	0.0		0.0		12.8		0.0	
	10.0	8.6	86.5 ± 1.6	8.0	80.3 ± 3.3	20.8	80.1 ± 1.7	9.1	91.2 ± 6.4
	20.0	18.4	91.8 ± 3.7	17.8	89.2 ± 5.5	29.2	82.2 ± 4.8	171.3	85.7 ± 4.5
	200.0	176.9	88.5 ± 4.5	156.7	78.4 ± 7.1	166.7	77.0 ± 3.2	173.2	86.7 ± 1.8
Sample 5	0.0	0.0		0.0		0.0		0.0	
	10.0	9.1	90.6 ± 2.3	9.7	97.2 ± 6.1	8.4	84.5 ± 4.9	8.1	81.3 ± 5.4
	20.0	19.8	99.2 ± 1.4	17.6	87.8 ± 1.3	17.7	88.3 ± 2.7	18.5	92.4 ± 4.6
	200.0	179.2	89.6 ± 5.4	187.0	93.5 ± 3.9	180.8	90.4 ± 5.6	173.8	86.9 ± 2.8

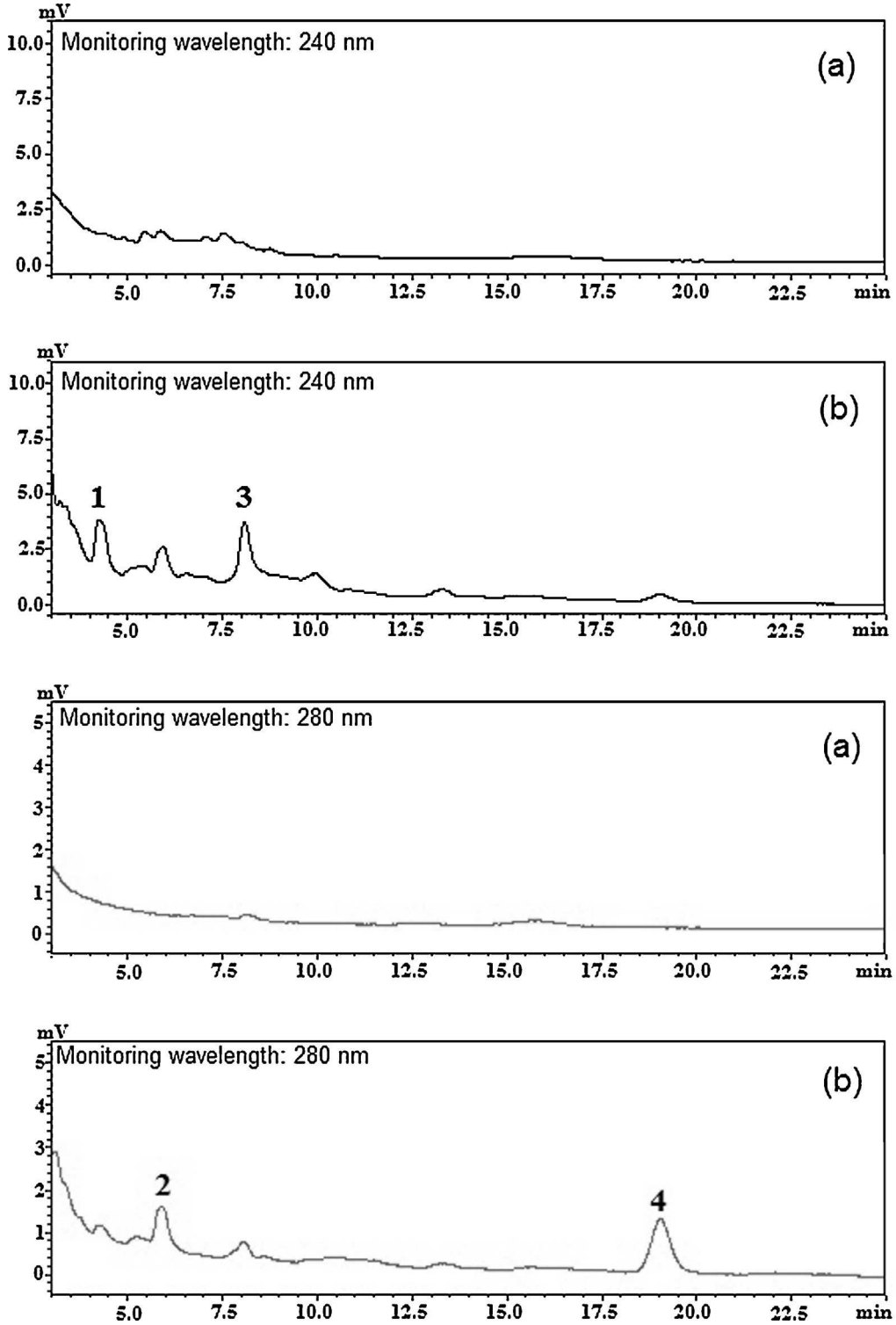

Fig. 8. The chromatograms of blank urine sample 1 (a) and spiked sample 1 (b); (1) 4, 4′-DADP; (2) 4-APT; (3) AN; and (4) 4-ABP. The pH value, 9; C_{18}-UMS NPs, 50 mg; extraction time, 20 min; desorption solvent, acetonitrile; desorption time, 3 min; desorption time, 1 min. Spiked concentration, 20.0 ng mL^{-1}.

The linearities of the aromatic amines were studied in real urine samples. No aromatic amines were found in the urine sample 1. Under the optimized conditions, calibration curves are established for aromatic amines by adding certain amount of aromatic amines into sample 1. The limits of detection (LODs) and quantification (LOQs) of the investigated compounds were estimated as the minimum concentration determined with a signal-to-noise ratio of 3 and 10, respectively. The linear ranges, calibration equations, correlation coefficients (r), LODs and LOQs are listed in Table 1. The results show that the present method has wide linear range, high sensitivity and good precision. Calibration curves of the analytes exhibit good linearity with correlation coefficient $r > 0.9992$. The LODs of the analytes are 0.88–1.3 ng mL^{-1}.

Table 4
Comparison with other reported methods for aromatic amines determination.

Analytes	Sample preparation step	Extraction time (min)	LOD (ng mL^{-1})	Recoveries (%)	Recycled	Ref.
4-Aminobiphenyl *O*-toluidine	$\text{Urine} \xrightarrow[80\ ^\circ\text{C}]{\text{HCl}} \text{conjugates} \xrightarrow{\text{NaOH}} \text{mixture} \xrightarrow{\text{internal standard}} \text{mixture} \xrightarrow{\text{totulene}} \text{extract} \xrightarrow[\text{re-extraction}]{\text{totulene}} \text{extract} \xrightarrow{N_2} \text{residue} \xrightarrow[\text{PFPA}]{\text{pyridine}} \text{derivatisation} \xrightarrow[\text{extraction}]{\text{potassium phosphate buffer}} \text{mixture} \xrightarrow[\text{centrifugation}]{\text{evaporation}} \text{supernatant} \xrightarrow[\text{evaporation}]{N_2} \text{analytical solution}$	126	0.1	–	No	[8]
Aromatic amines	$\text{Urine} \xrightarrow[80\ ^\circ\text{C}]{\text{HCl}} \text{conjugates} \xrightarrow{\text{NaOH}} \text{mixture} \xrightarrow{\text{MES buffer}} \text{mixture} \xrightarrow{\text{n-hexane}} \text{extract} \xrightarrow[\text{re-extraction}]{\text{n-hexane}} \text{extract} \xrightarrow[\text{centrifugation}]{} \text{supernatant} \xrightarrow[\text{pentafluoropropionic anhydride}]{\text{NaOH}} \text{derivatisation} \xrightarrow{\text{phosphate}} \text{mixture} \xrightarrow[\text{centrifugation}]{} \text{supernatant} \xrightarrow{\text{toluene}} \text{mixture} \xrightarrow[\text{evaporation}]{N_2} \text{analytical solution}$	140	0.05–2	70–125	No	[22]
Heterocyclic aromatic amines	$\text{Urine} \xrightarrow{\text{NaOH}} \text{mixture} \xrightarrow{\text{magnetic bar}} \text{mixture} \xrightarrow[\text{extraction}]{\text{hollow fibre}} \text{extract} \xrightarrow{\text{transfer}} \text{extract} \xrightarrow{\text{acceptor solution}} \text{analytical solution}$	90	0.1–0.5	–	No	[23]
Aromatic amines	$\text{Urine} \xrightarrow{\text{phosphate buffer}} \text{mixture} \xrightarrow[\text{extraction}]{C_{18}\text{-UMS NPs}} \text{adsorbate} \xrightarrow[\text{elution}]{\text{acetonitrile}} \text{eluate} \xrightarrow[\text{evaporation}]{N_2} \text{analytical solution}$	21	0.88–1.3	77.0–99.2	Yes	This method

The intra-day and inter-day precision and accuracy of the method were evaluated by assaying spiked urine samples at three concentration levels (10, 20 and 250 ng mL^{-1}) of the targets in the same and six consecutive days, respectively. The recoveries and relative standard deviations (RSDs) of the intra-day and inter-day precision are summarized in Table 2. The intra-day and inter-day recoveries are in the range of 91.8–105.5% and 88.7–102.8%, respectively.

3.5. Analysis of urine samples

To validate the feasibility of the method, five real urine samples were analyzed. Among the five urine samples, the four aromatic amines were undetectable in sample 1, 2, 3 and 5. The concentration of AN in sample 4 is 12.8 ng mL^{-1}. The recoveries of aromatic amines were studied by adding a certain amount of aromatic amines at three concentrations (10, 20 and 200 ng mL^{-1}) into urine samples. The recoveries for the target compounds are listed Table 3. The recoveries of AN, 4-ABP, 4,4′-DADP and 4-APT are in the range of 70.7% to 99.2%. The results indicate that the recoveries for the analytes are satisfactory. Fig. 8 shows liquid chromatograms of urine sample and spiked urine sample at the analytes concentration of 20.0 ng mL^{-1}.

3.6. Comparison of the MSPE method with other methods used in the literatures

A comparison between the proposed method and other methods [10,25,26] reported in literature was made, and the results are shown in Table 4. The results indicate that there is no significant difference in the recoveries obtained by different methods. In the previous methods, expensive apparatus and multiple operation procedures should be required. In the MSPE method, the extraction and clean-up steps could be fulfilled synchronously by mixing the magnetic adsorbents and urine sample at room temperature. It simplified the operation procedure and reduced the analysis cost. Meanwhile, the magnetic adsorbents possessed superparamagnetism properties, which enabled them to be completely isolated from matrix in a short amount of time (shorter than 1 min) by a strong magnetic. Rapid separation rate and escape from the time-consuming column passing shortened the analysis time greatly. Results were satisfactory.

4. Conclusions

In this work, C_{18}-UMS NPs with high magnetic responsivity were synthesized and successfully applied for the extraction and enrichment of aromatic amines in urine sample. Aromatic amines were extracted from urine sample rapidly and adsorbed to C_{18}-UMS NPs. Under an external magnetic field, the C_{18}-UMS NPs were rapidly isolated from urine matrix promptly without additional centrifugation or filtration. The adsorbed aromatic amines were easily desorbed with acetonitrile. Good recoveries and precision of this method were obtained. It is anticipated that the C_{18}-UMS NPs have great analytical potential for the separation, enrichment and purification of organic compounds from urine matrix.

Acknowledgements

This work was supported by National Natural Science Foundation of China (Nos. 20727003, 21075049, 21105037), Program for New Century Excellent Talents in University (No. NECT-10-0443) and Science and Technology Developing Foundation of Jilin Province (Nos. 20100356, 20110162).

Appendix A. Supplementary data

Supplementary data associated with this article can be found, in the online version, at http://dx.doi.org/10.1016/j.jchromb.2013.12.008.

References

[1] K.I. Kitahara, S. Okuya, I. Yoshihama, T. Hanada, K. Nagashima, S. Arai, J. Chromatogr. A 1216 (2009) 7409.
[2] S. Erdemir, M. Bahadir, M. Yilmaz, J. Hazard. Mater. 168 (2009) 1170.
[3] Chinese National Surface Water Quality Standard, General Administration of Quality Supervision, Inspection and Quarantine of the People's Republic of China (2002) GB 3838-2002, Chinese National Surface Water Quality Standard, 2002.
[4] K. Reddy-Noone, A. Jain, K.K. Verma, Talanta 73 (2007) 684.
[5] X. Zhao, Y. Suo, J. Sep. Sci. 31 (2008) 646.
[6] Z. Karim, Q. Husain, Int. Biodeterior. Biodegrad. 63 (2009) 587.
[7] J.G. Lavandeira, C.S. Petinal, E. Blanco, R. Cela, Anal. Bioanal. Chem. 397 (2010) 751.
[8] Chinese National General Safety Technical Code for Textile Products, General Administration of Quality Supervision, Inspection and Quarantine of the People's Republic of China (2003) GB 18401-2003, Chinese National General Safety Technical Code for Textile Products, 2003.
[9] P. Vineis, R. Pirastu, Cancer Cause Control 8 (1997) 346.
[10] T. Schettgen, K. Heinrich, T. Kraus, M. Gube, Arch. Toxicol. 85 (2011) 127.
[11] B. Takkouche, M. Etminan, A. Montes-Martinez, JAMA 293 (2003) 1162.
[12] G. Grimmer, G. Dettbarn, A. Seidel, J. Jacob, Sci. Total Environ. 247 (2000) 81.
[13] Y.C. Wu, S.D. Huang, Anal. Chem. 71 (1999) 310.
[14] A. Dasgupta, J. Chromatogr. B 716 (1998) 354.
[15] X.L. Zhang, H.Y. Niu, S.X. Zhang, Y.Q. Cai, Anal. Bioanal. Chem. 397 (2010) 791.
[16] F. Yang, R. Shen, Y. Long, X. Sun, F. Tang, S. Yao, J. Environ. Monit. 13 (2011) 440.
[17] Y.F. Huang, Y. Li, Y. Jiang, X.P. Yan, J. Anal. At. Spectrom. 25 (2010) 1467.
[18] X. Zhang, H. Niu, Y. Pan, Y. Shi, Y. Cai, Anal. Chem. 82 (2010) 2363.
[19] Y. Liu, L. Jia, Microchem. J. 89 (2008) 72.
[20] A. Afkhami, R. Moosavi, T. Madrakian, Talanta 82 (2010) 785.
[21] Q. Zhang, F. Yang, F. Tang, K. Zeng, K. Wu, Q. Cai, S. Yao, Analyst 135 (2010) 2426.
[22] H. Parham, N. Rahbar, Talanta 80 (2009) 664.
[23] X. Zhao, Y. Shi, T. Wang, Y. Cai, G. Jiang, J. Chromatogr. A 1188 (2008) 140.
[24] Q. Gao, D. Luo, J. Ding, Y.Q. Feng, J. Chromatogr. A 1217 (2010) 5602.
[25] T. Weiss, J. Angerer, J. Chromatogr. B 778 (2002) 179.
[26] F.U. Shah, T. Barri, J.A. Jonsson, K. Skog, J. Chromatogr. B 870 (2008) 203.

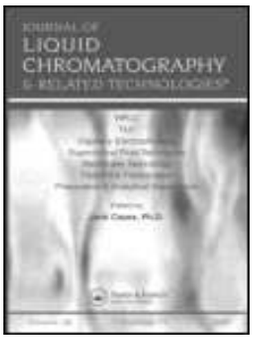

Taylor & Francis
Taylor & Francis Group

Journal of Liquid Chromatography & Related Technologies

ISSN: 1082-6076 (Print) 1520-572X (Online) Journal homepage: https://www.tandfonline.com/loi/ljlc20

C_{18}-Functionalized Magnetic Silica Nanoparticles for Solid Phase Extraction of Microcystin-LR in Reservoir Water Samples Followed by HPLC-DAD Determination

Jiping Ma, Fengli Yan, Fengxi Chen, Lianhua Jiang, Jinhua Li & Lingxin Chen

To cite this article: Jiping Ma, Fengli Yan, Fengxi Chen, Lianhua Jiang, Jinhua Li & Lingxin Chen (2015) C_{18}-Functionalized Magnetic Silica Nanoparticles for Solid Phase Extraction of Microcystin-LR in Reservoir Water Samples Followed by HPLC-DAD Determination, Journal of Liquid Chromatography & Related Technologies, 38:6, 655-661, DOI: 10.1080/10826076.2014.936611

To link to this article: https://doi.org/10.1080/10826076.2014.936611

Published online: 22 Aug 2014.

Journal of Liquid Chromatography & Related Technologies, 38: 655–661, 2015

ISSN: 1082-6076 print/1520-572X online
DOI: 10.1080/10826076.2014.936611

Taylor & Francis
Taylor & Francis Group

C_{18}-Functionalized Magnetic Silica Nanoparticles for Solid Phase Extraction of Microcystin-LR in Reservoir Water Samples Followed by HPLC-DAD Determination

JIPING MA,[1] FENGLI YAN,[1] FENGXI CHEN,[2] LIANHUA JIANG,[1] JINHUA LI,[3] and LINGXIN CHEN[3]

[1]*Key Lab of Environmental Engineering in Shandong Province, School of Environment & Municipal Engineering, Qingdao Technological University, Qingdao, China*
[2]*School of Chemical Engineering & Pharmacy, Wuhan Institute of Technology, Wuhan, China*
[3]*Key Laboratory of Coastal Environmental Processes and Ecological Remediation, Yantai Institute of Coastal Zone Research, Chinese Academy of Sciences, Yantai, China*

In this study, C_{18}-functionalized magnetic silica nanoparticle ($Fe_3O_4@SiO_2@C_{18}$ MNPs) based magnetic solid phase extraction (MSPE) was successfully developed for the determination of microcystin-LR (MC-LR) in reservoir water samples followed by high performance liquid chromatography–diode array detection (HPLC–DAD). After the extraction, the adsorbent can be conveniently and rapidly separated from aqueous samples by an external magnet. The main factors influencing the extraction efficiency including the amount of the MNPs, the extraction time, the pH of sample solution, and desorption conditions were optimized to obtain high recoveries and extraction efficiency. High enrichment factor 500 was attained. Under the optimized experimental conditions, the calibration curve of MC-LR was linear in the range of 0.1–10.0 μg/L with correlation coefficients (r^2) 0.9996. Limit of detection (LOD, S/N = 3) of the method was 0.056 μg/L. The developed method was successfully applied to the determination of MC-LR in reservoir water samples. The method recoveries were obtained ranging from 73.3–104% for three spiked concentrations, with the relative standard deviations (RSD) of 2.90–4.30%. The developed $Fe_3O_4@SiO_2@C_{18}$ MNPs-based MSPE coupled with HPLC–DAD demonstrated excellent sensitivity and repeatability, simplicity, rapidity, and ease of operation, as well as practical applicability.

Keywords: C_{18}-functionalized magnetic silica nanoparticles, HPLC-DAD, magnetic solid phase extraction, microcystins, preconcentration, water samples

Introduction

In recent years, cyanobacterial blooms occur frequently in eutrophic bodies of freshwater. A variety of toxins can be released by algae cells rupture. Among them, microcystins (MCs) have the highest frequency, the largest quantity, and produce the most serious type of harm.[1] MCs are a family of hepatic toxins, which have been considered as potential tumor promoters. They are also responsible for the poisoning death of wild animals, livestock, poultry, and so forth.[2] MCs are a kind of monocyclic heptapeptide with biological activity. Its general structure (Figure 1) is cyclo (D-Ala-X-D-MeAsp-Z-Adda-D-Glu-Mdha) and relative molecular weight is about 1000.[3] There are more than 60 MCs isoforms that have been identified.[4] MC-LR is one of the most frequent variants. Owing to the increased concerns about the public health risks associated with MCs intake, the WHO recommends a provisional level of 1 μg/L for MC-LR concentration in drinking water.[5]

Address correspondence to: Jiping Ma, Key Lab of Environmental Engineering in Shandong Province, School of Environment & Municipal Engineering, Qingdao Technological University, Qingdao, 266033, China, E-mail: majiping2012@163.com

Color versions of one or more of the figures in the article can be found online at www.tandfonline.com/ljlc.

To develop a simple, sensitive, and rapid detection method for MCs is necessary and important. The most widespread analytical techniques for MCs include commercial enzyme-linked immunosorbent assays (ELISA),[6] liquid chromatography with UV detection (HPLC-UV),[7] capillary electrophoresis (CE),[8] and liquid chromatography–mass spectrometry (LC–MS).[9–11] LC–MS offers the advantages of providing specificity and good sensitivity, however, the expensive cost makes it difficultly popularize. HPLC is a powerful tool to separate microcystins; however, UV detector cannot provide the similar sensitivity and selectivity to LC–MS without enrichment prior to analysis, as the concentration of MCs in water is low (usually at the level of ng/L–μg/L). Therefore, pretreatment techniques are needed for the enrichment and clean-up of MCs in environmental samples, in order to achieve the ideal determination sensitivity and effectively eliminate contaminants from complex samples. Up to now, the reported pretreatment techniques for MCs include solid-phase extraction (SPE),[12–16] solid-phase microextraction (SPME),[17] cloud point extraction (CPE),[18,19] and so on. Among them, SPE is typically utilized. An HPLC method with UV detection after SPE was published as an ISO 20179 international standard.[12] SPE is also listed as the National Standard Method of China for determination of MCs in water.[20] Compared to liquid–liquid extraction, SPE has higher enrichment efficiency, uses less organic solvents, and does not produce

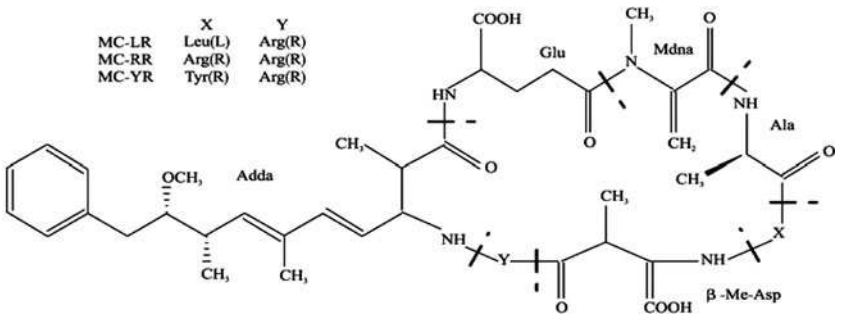

Fig. 1. Structure of microcystins.

emulsification phenomenon. This method is easy to realize automation.[21] However, the porous structure of the stationary phase is easily jammed by the complex samples containing colloid or solid granules, resulting in the lower column capacity and extraction efficiency. Moreover, for a large volume of water sample, the pretreatment process needs a long time, typically 2–4 h for 1 L water sample. Compared with SPE method, SPME has the following advantages: without organic solvent, no need for clean-up procedures, simple operation, and short analysis time.[22] However, SPME fibers are comparatively expensive and have a limited lifetime, as they tend to degrade with repeated usage.[23]

Recently, sample extraction by magnetic nanoparticles (MNPs) has gained increasing attention due to significantly higher surface area-to-volume ratio and superparamagnetic property.[24–28] The Fe_3O_4 nanoparticles adsorbed with target compounds can be easily collected by an external magnetic field outside the extraction container without additional centrifugation or filtration of the sample.[29] To avoid alteration of the magnetic properties of magnetite or its oxidation, Fe_3O_4 nanoparticles are often coated with silica. The silica coating was subsequently functionalized with organosilanes and/or affinity ligands in order to enable the selective extraction of organic contaminants. The $Fe_3O_4@SiO_2$ nanoparticles modified with alkyl C_{18}($Fe_3O_4@SiO_2@C_{18}$) are mostly applied, such as for the determination of methylprednisolone in rat plasma,[30] ergosterol in cigarettes,[31] polycyclic aromatic hydrocarbons in aqueous samples,[25] and organophosphorus pesticides in environmental water.[32]

Despite the high concentrating potential of nanomaterial and the ease of handling MNPs, no MNPs-based SPE have been used to concentrate microcystins in water. The aim of this work was to develop a sensitive analytical method to determine MC-LR in environmental water samples. Laboratory-made $Fe_3O_4@SiO_2@C_{18}$ MNPs were utilized for SPE procedure followed by HPLC analysis. Several key influence factors including the amount of the MNPs, the extraction time, the pH of sample solution, and desorption conditions were optimized to obtain high recoveries and extraction efficiency. The method was demonstrated to be applicable for the analysis of MC-LR in real reservoir water samples.

Experimental

Reagents and Materials

Methanol (HPLC grade) was purchased from Merck (Darmstadt, Germany). Trifuoroacetic acid (TFA) of HPLC grade was from Dima Tech. (USA). Water was purified to 18.2 MΩ on a Synergy 185 ultrapure water system (Millipore, USA). MC-LR (10 μg/mL) standard solution was from Institute of Hydrobiology, CAS (China), which was stored and refrigerated at − 20°C. The working standard solution was freshly prepared by diluting the standard solution with ultrapure water to required concentrations. $FeCl_3 \cdot 6H_2O$, ethylene glycol, ammonium hydroxide, absolute ethyl alcohol, and NaAc were analytical reagents. Polyethylene glycol (Alfa Aesar), trichloro (octadecyl) silane (Alfa Aesar), TEOS, trimethylchorosilane, and triethylamine (Alfa Aesar) were used. Toluene was HPLC grade.

Preparation of C_{18}-Functionalized Magnetic Silica Nanoparticles

The C_{18}-functionalized magnetic silica nanoparticles ($Fe_3O_4@SiO_2@C_{18}$ MNPs) were synthesized according to the previously reported method.[25] The route for preparation of $Fe_3O_4@SiO_2@C_{18}$ MNPs was illustrated in Figure 2. First, the magnetic Fe_3O_4 microspheres were synthesized by a solvothermal reduction method; second, the Fe_3O_4 microspheres were modified with TEOS; and third, the C_{18} chain was bonded to the surface of silica gel modified magnetic microspheres through the Si–O–Si combination.

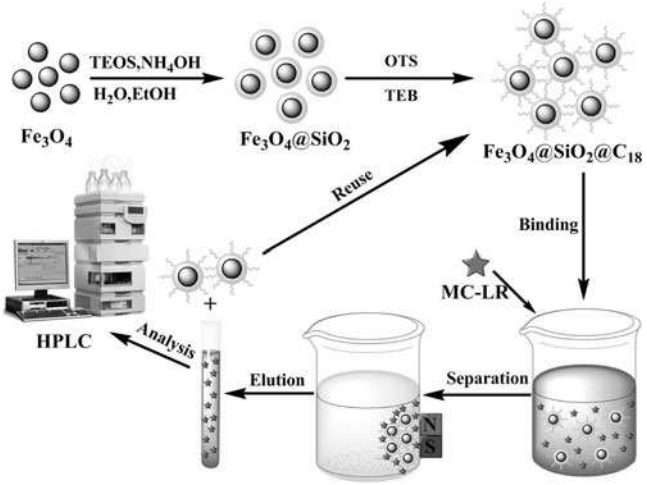

Fig. 2. Schematic synthesis of C_{18}-functionalized magnetic silica nanoparticles ($Fe_3O_4@SiO_2@C_{18}$ MNPs), and magnetic separation procedure.

Apparatus and Measurement

The characterizations of magnetic silica NPs and C_{18}-functionalized magnetic silica nanoparticles were conducted on a Tescan XM 5136 scanning electron microscope (SEM, Tescan, Czech Republic) and Fourier-transform infrared spectrometry (FT-IR, Frontier, Perkin Elmer, USA).

Experiments were performed on an Agilent 1100 liquid chromatographic system, consisting of a quaternary delivery pump, an auto-sampler with a 100 μL loop, a thermostated column compartment, and a DAD detector. A personal computer equipped with an Agilent ChemStation program for HPLC was used to process the chromatographic data. The analytical column was Agela Vensuil MP-C_{18} (250×4.6 mm i.d., 5 μm), which was used for analysis of MC-LR at room temperature. The sample injection volume was 20 μL. The absorbance was monitored at 238 nm. The mobile phase was methanol–water (0.05% TFA) (60:40, v/v). The flow rate was 1 mL/min.

Magnetic Solid Phase Extraction (MSPE) Procedures

The 30 mg magnetic C_{18} microspheres were put into a 2-L beaker and firstly cleaned and activated with 5 mL methanol and 10 mL distilled water in sequence. The beaker was placed in an ultrasound bath for 1 min. Then, 1 L of MC-LR aqueous solution was added into the beaker. The mixture was sonicated at room temperature for 7 min to form a homogeneous dispersion solution. Then, magnetic C_{18} microspheres adsorbed MC-LR were separated rapidly from the solution under a strong external magnetic field. After discarding the supernatant solution, MC-LR was eluted from the magnetic C_{18} microspheres with 2×5 mL of methanol sonicated at room temperature for 3 min. The effluents were collected into a test tube and condensed to dryness under a gentle flow of nitrogen at room temperature and re-dissolved with 0.2 mL methanol. The resulting solution was then transferred to double layer silicone-Teflon sept vials for autosampler and analysis by HPLC-DAD. The MSPE process is schematically shown in Figure 2.

Results and Discussion

Characterization of the C_{18}-Functionalized Magnetic Silica Nanoparticles

The magnetic C_{18} microspheres were strong enough to be easily separated by an external magnetic field, as seen from Figure 3. The size and shape of the prepared microspheres were examined by SEM. As observed, the prepared magnetic C_{18} microspheres are homogeneous and spherical, having uniform sizes in the range of 100–190 nm (Figure 3).

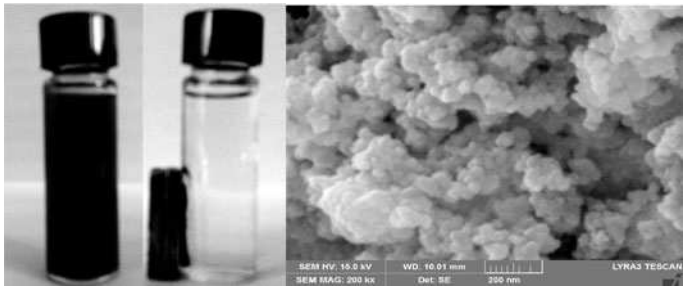

Fig. 3. The dispersion (left) and separation (right) process; SEM image of the $Fe_3O_4@SiO_2@C_{18}$ MNPs.

FT-IR spectroscopy was applied to characterize the magnetic silica microspheres before and after modification with a silane coupling agent. Figure 4 shows the FT-IR spectra of Fe_3O_4, $Fe_3O_4@SiO_2$, and $Fe_3O_4@SiO_2@C_{18}$. The absorption peak at 580 cm^{-1} is from Fe–O–Fe vibration of magnetite, and 1080 cm^{-1} is attributed to the Si–O–Si stretching vibration of silica layer formed on the surface of magnetite particles. After surface modification, the new emergence of absorption peaks at 2921 cm^{-1} and 2853 cm^{-1} is ascribed to C–H originated from silane coupling agent, suggesting the alkyl groups have been successfully grafted on the surface of magnetic silica microspheres.

Optimization of MSPE Procedure

Recovery was the best indicator of MSPE method. The recoveries of MC-LR in MSPE process was mainly subjected to several factors including the amount of the MNPs, the extraction time, the pH of sample solution, and desorption conditions. In this study, these major factors were investigated using a spiked ultrapure water sample (0.4 μg/L), and all the optimization experiments were conducted three times.

Effect of the Amount of Adsorbent

The amount of the adsorbent was investigated such that the adsorbent not only adsorbs sufficient analysts but also remains utilized. Amounts of 10, 20, 30, 40, and 50 mg magnetic C_{18} microspheres were discussed and the results are shown in Figure 5A. As shown, the extraction recovery for the analytes increased rapidly when the $Fe_3O_4@SiO_2@C_{18}$ MNPs amount was increased from 10 to 30 mg and then remained almost constant when the amount of the adsorbent was above 30 mg. Based on the aforementioned results, the addition of 30 mg $Fe_3O_4@SiO_2@C_{18}$ MNPs was employed for the following studies.

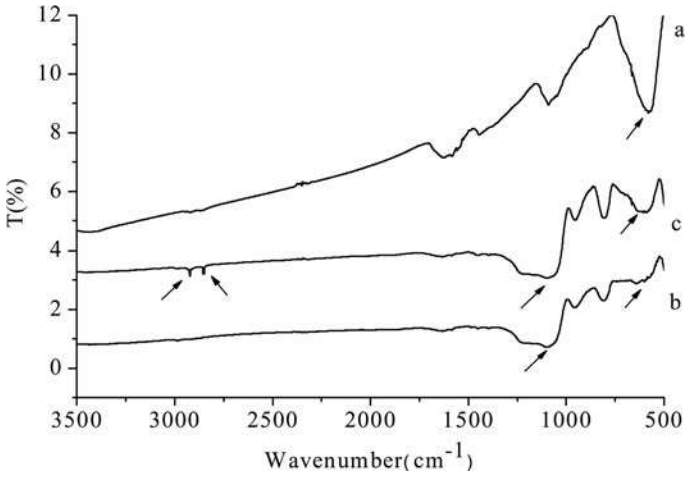

Fig. 4. FT-IR spectra of (a) Fe_3O_4; (b) $Fe_3O_4@SiO_2$; and (c) $Fe_3O_4@SiO_2@C_{18}$.

Extracting Time

In the MSPE process, the extraction time is one of the prime factors that influence the extraction of the analytes. The effect of extraction time on the adsorption was investigated from 3-20 min. As shown in Figure 5B, when the sample solution was sonicated for 7 min, the extraction recoveries of MC-LR reached the maximum. This result suggests that the adsorption equilibrium can be achieved at about 7 min. Therefore, an extraction time of 7 min was selected.

Desorption Conditions

The type and volume of elution solvent are vital for the extraction efficiency. Thus, the choice of elution solvent and its optimum volume should be carefully taken into account. Desorption of the analytes from the magnetic adsorbents was studied using 10 mL of three different solvents including methanol, 99.9% methanol (methanol: TFA (13.07 mol/L) = 99.9:0.1, V/V) and 80% methanol (methanol: TFA (13.07 mol/L) = 80:20, V/V). The recoveries of MC-LR eluted by methanol, 99.9% methanol, and 80% methanol were 68.6%, 72.4%, and 58.1%, respectively. The eluting power of 99.9% methanol was the strongest among them. Hence, 99.9% methanol was chosen as the elution solvent.

Moreover, the influence of volume of 99.9% methanol was tested. The recoveries of MC-LR eluted by 5, 10, and 15 mL of 99.9% methanol were 56.7%, 72.4%, and 74.1%, respectively. Although the highest recovery was obtained by 15 mL of 99.9% methanol elution solvent, the concentration time was longer. Finally, 10 mL of 99.9% methanol was adopted for eluting MC-LR for further work.

In addition, the desorption time was also investigated from 1 to 5 min under sonication. As shown in Figure 5C, the result indicated that desorption time had an obvious effect on the extraction efficiency. The extraction recovery for the analytes increased rapidly when the desorption time was increased from 1 to 3 min and then remained almost constant when the desorption time was 3 min. Thus, the desorption time was selected as 3 min. This result indicated that the desorption process was quick and efficient. However, for the adsorption process, the mass transfer of the analytes from water samples to the solid adsorbent

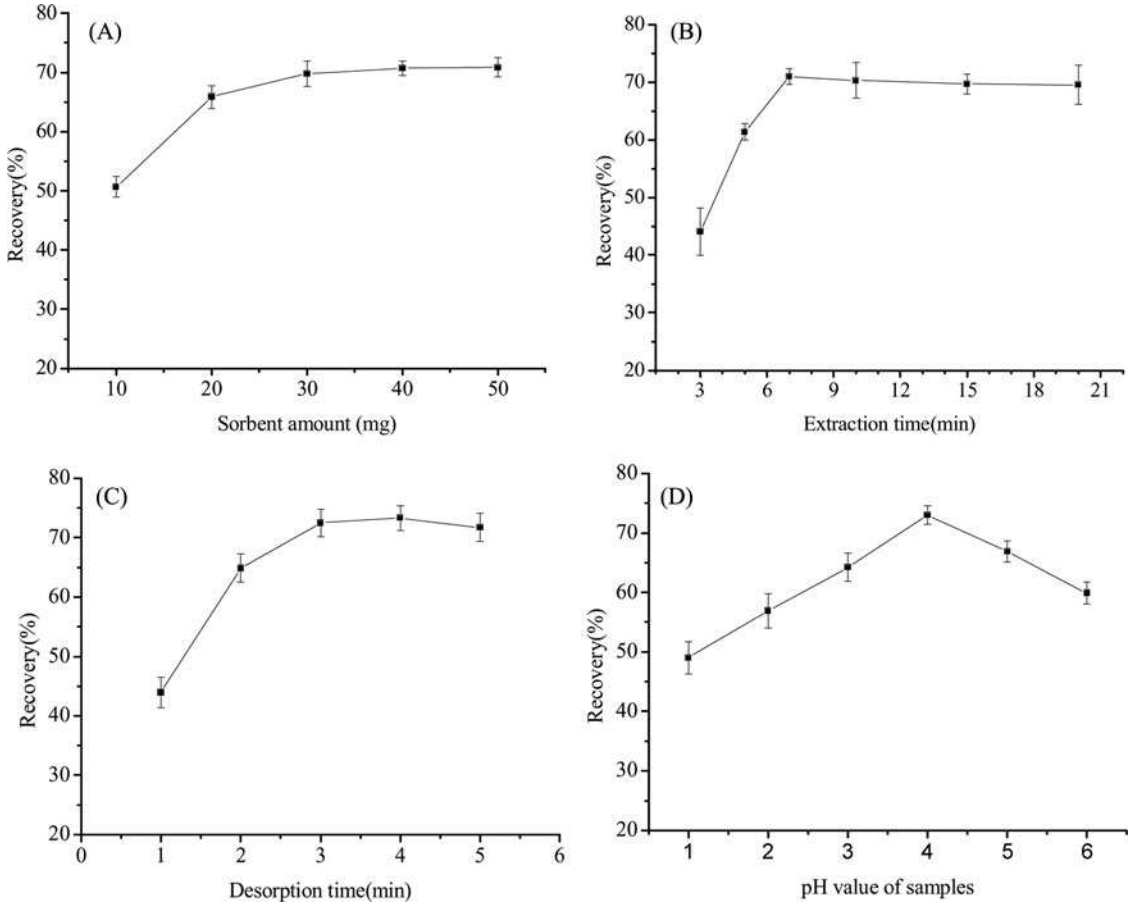

Fig. 5. Effect of (A) the amount of the magnetic C_{18} microspheres, (B) extraction time, (C) desorption time, and (D) solution pH on the extraction efficiency of MNPs-based SPE for MC-LR. Extraction conditions: sample volume, 1.0 L; concentration of MC-LR, 0.4 μg/L; (a) extraction time, 7 min; sample pH, 4; desorption solvent, 2 × 5 mL of methanol; desorption time, 3 min; (b) the amount of the magnetic C_{18} microspheres, 30 mg; desorption time, 3 min; sample pH, 4; desorption solvent, 2 × 5 mL of methanol; (c) the amount of the MNPs, 30 mg; extraction time, 7 min; sample pH, 4; desorption solvent, 2 × 5 mL of methanol; (d) the amount of the MNPs, 30 mg; sample volume, 1 L; extraction time, 7 min; desorption solvent, 2 × 5 mL of methanol; desorption time, 3 min.

was much slower. Therefore, the desorption time was much faster than the extraction time (adsorption, 7 min).

Effect of Solution pH

MC-LR is potentially ionizable compounds. Taking into account the lipophilic phase of the magnetic C_{18} microspheres surface, the neutral (i.e., not ionized) forms of the compounds are expected to be easily extracted. In this sense, pH values ranging from 1 to 6 were studied. As can be seen in Figure 5D, the extraction recovery for MC-LR increased when $pH < 4$, followed by decreasing when $pH > 4$. The highest signals were obtained when the samples were prepared at pH 4. The effect of sample pH on the extraction efficiency was consistent with the retention factor K of MC-LR on C_{18}.[33] At pH 4, a major portion of the MC-LR was protonated (the neutral form), resulting in stronger adsorption on the surface of the $Fe_3O_4@SiO_2@C_{18}$ MNPs. Therefore, a pH value of 4 was selected for further experiments.

Salt Effect

To investigate the salt effect on the extraction of the MC-LR, NaCl was used to adjust the solution salinity. The results that the peak areas for MC-LR did not obviously increase as the concentration of NaCl increased from 0% to 30%. Therefore, no NaCl was added in the following extractions.

Analytical Performance

Under the aforementioned optimal conditions, the analytical performance of the proposed method was assessed. Six standard solutions with different concentration (0.1, 0.2, 0.5, 1.0, 2.0, 3.0, 5.0, and 10.0 μg/L for MC-LR) were obtained by serial dilution with ultrapure water from the standard solution. Working curves were obtained by a least-squares linear regression analysis of the peak area of the analytes versus analyte concentrations. The method presented excellent linearity in the range of 0.1–10.0 μg/L for MC-LR with the correlation coefficient (r^2) of 0.9996. The obtained linear regression equation was $y = 120.15x - 2.2056$, where y means the peak area and x stands for the concentration of MC-LR. The limit of detection (LOD) calculated by analyzing the spiked sample using a signal-to-noise ratio of 3 was 0.056 μg/L. The limit of quantitation (LOQ) of 0.18 μg/L was achieved for MC-LR. WHO recommended a provisional level of 1 μg/L for MC-LR concentration in drinking water. As a result, the developed MSPE-HPLC–DAD method proved potentially applicable for MC-LR determination in drinking water samples. On the other hand, the intra-day and inter-day precisions in terms of peak area obtained on the basis of six injections were investigated. The relative standard deviations (RSDs) for MC-LR at 0.5 and 5 μg/L based on intra-day precision were less than 5.02% and 3.95%, respectively, while the inter-day remained under 6.15% and 8.22%, respectively. Moreover, a high enrichment factor of 500 was obtained. Therefore, the $Fe_3O_4@SiO_2@C_{18}$ MNPs-based MSPE coupled with HPLC–DAD could sensitively and accurately quantify the MC-LR.

Moreover, the reusability of the $Fe_3O_4@SiO_2@C_{18}$ MNPs was examined. In order to investigate the possibility of the reuse, the $Fe_3O_4@SiO_2@C_{18}$ MNPs were reused for three adsorption-desorption cycles, and nearly constant recovery values were obtained with relative error less than 3%. Also, the FT-IR spectra of the $Fe_3O_4@SiO_2@C_{18}$ MNPs for the first use and after the third use were consistent. Therefore, the results showed the magnetic separation under an external magnetic field could easily reach, and the stable $Fe_3O_4@SiO_2@C_{18}$ MNPs could effectively extract MC-LR at least three repeated cycles without obvious decrease of recovery.

Comparison of Different Analytical Methods

Table 1 shows the comparison of different analytical methods for the determination of MC-LR. The higher sensitivity achieved is 0.02 μg/L based on an on-line trace enrichment SPE system coupled with LC–DAD.[13] As it is difficult to conduct clean-up in the on-line enrichment system, interference will strongly disturb the accuracy of the results. Although the analysis of MC-LR by HPLC–MS/MS[9,17,18] can provide lower LODs, the instrument is expensive so as to difficultly popularize. The method developed in our current study presented the lower LODs. The method displays excellent reusability and rapid simple magnetic separation, less than 15 min by just using a magnet. On the other hand, compared to previous reports which also employed MSPE,[24,31,34] the method presented herein has the advantages of larger sample volume (1 L, most reports using lower volume than 350 mL) and higher enrichment factors (500).

Applications of the MSPE to Water Samples

In order to evaluate the method applicability, the water sample collected from Qingdao Jihongtan reservoir was analyzed. Prior to use, the water samples were filtered through a 0.45-μm

Table 1. Method comparisons for analysis of MC-LR

Methods	Matrix	Adsorbent	LODs (μg/L)	Sample pretreatment time (min)	Ref.
On-line SPE–HPLC/DAD	Surface water	Zorbax CN	0.02	~50	[13]
SPE–LC/MS/MS	Surface water	Waters Oasis HLB	2.6 ng/L	>4 h	[9]
SPME–HPLC/QTOF/MS	Lake-water	CW–TPR fiber	0.8	>45	[17]
CPE–HPLC/MS/MS	Natural waters	Ionic-liquid	0.03	~15	[18]
MSPE–HPLC/DAD	Reservoir water	$Fe_3O_4@SiO_2@C_{18}$ MNPs	0.056	<15	This work

CPE, CPE-cloud point extraction.

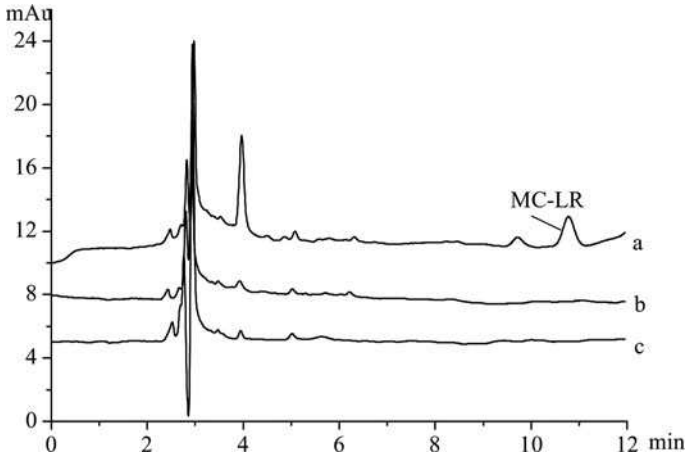

Fig. 6. HPLC-DAD chromatograms of reservoir water samples (a) with spiking MC-LR after MSPE, (b) without spiking MC-LR after MSPE, and (c) no pretreatment and without spiking MC-LR. The spiked concentration of MC-LR standard was 1.0 μg/L. Extraction conditions: sample volume, 1.0 L; the amount of the MNPs, 30 mg; sample volume, 1 L; extraction time, 7 min; desorption solvent, 2 × 5 mL of methanol; desorption time, 3 min; sample pH, 4.

Table 2. Determination results of MC-LR and method recoveries in real water samples

Sample	Spiked (μg/L)	Found (μg/L)	Recovery (% ±RSD, $n = 3$)
	0	ND	–
	0.500	0.521	104 ± 2.90
	1.000	0.747	74.7 ± 4.30
1	4.000	2.930	73.3 ± 3.50

ND, Not detected.

membrane. As seen from Figure 6, no MC-LR was detected in the water sample. The recoveries were obtained by spiked Qingdao Jihongtan reservoir water samples with 0.500, 1.00, and 4.00 μg/L of MC-LR, respectively. The recoveries and RSDs of spiked Jihongtan reservoir water sample were averaged from three replicate runs, as shown in Table 2. The recoveries ranged from 73.3–104%, with RSDs in the range of 2.90–4.30%. In addition, another reservoir water collected in June was studied, a possible eutrophic water sample. As expected, the endogenous MC-LR was detected, 0.51 μg/L. Fortunately, the tested reservoir water sample also satisfied the drinking water quality as the value was lower than the regulated level of 1 μg/L for MC-LR by WHO. Therefore, the developed MSPE using $Fe_3O_4@SiO_2@C_{18}$ MNPs as adsorbents followed by HPLC–DAD proved practically applicable to MC-LR analysis in reservoir water samples.

Conclusion

In conclusion, a simple, sensitive, and robust $Fe_3O_4@SiO_2@C_{18}$ MNPs-based MSPE method was successfully developed for the determination of MC-LR in reservoir water samples followed by HPLC–DAD. Good extraction efficiency and high enrichment factor were obtained for MC-LR. The LOD and LOQ were 0.056 μg/L and 0.18 μg/L, respectively. The LOQ was significantly lower than the provisional guideline value established by the WHO for MC-LR concentrations in drinking water (1.0 μg/L). The pretreatment time was significantly shorter, less than 15 min, compared to conventional SPE (2–4 h). Additionally, the assay needs no complicated devices. The developed MSPE-HPLC–DAD method provided great potential to analyze practical water samples.

Funding

The authors acknowledge the support of the National Natural Science Foundation of China (21107057, 51078193), the Natural Science Foundation of Shandong Province (ZR2010BL024), the Taishan Scholar Construction Project Special Foundation (2010016010), and the Special Foundation of Central Financial Support to Local Colleges and Universities (201020029).

References

1. Duy, T. N.; Lam, P. K. S.; Shaw, G. R. Toxicology and Risk Assessment of Freshwater Cyanobacterial (Blue-Green Algae) Toxins in Water. *Rev. Environ. Contam. Toxicol*. **2000**, *163*, 113–186.
2. Vasconcelos, V. M.; Pereira, E. Cyanobacteria Diversity and Toxicity in a Wastewater Treatment Plant (Portugal). *Water. Res*. **2001**, *35*, 1354–1357.
3. Kunimitsu, K. Chemistry and Toxicology of Cylic Hepatapetide Toxins, the Mi-crocystins from Cyanobacteria. *Microbiol. Cult. Coll*. **1994**, *10*, 5–33.
4. Sivonen, K.; Jones, G. Cyanobacterial Toxins. In *Toxic Cyanobacteria in Water: A Guide to Their Public Health Consequences, Monitoring and Management*; Chorus, I., Bartram, J. Eds., E&FN Spon: London, 1999; Vol. 41.
5. Falconer, I.; Bartram, J.; Chorus, I.; Kuiper-Goodman, T.; Utkilen, H.; Burch, M.; Codd, J. Safe Levels and Safe Practices. In *Toxic Cyanobacteria in Water–a Guide to Their Public Health Consequences Monitoring and Management*, Chorus, I., Bartram, J. Eds., on behalf of WHO, Spoon Press: London, 1999; 155–178.
6. Chu, F. S.; Huang, X.; Wei, R. D. Enzyme-Linked Immunosorbent Assay for Microcystins in Blue-Green Algal Blooms. *J. Assoc. Off. Anal. Chem*. **1990**, *73*, 451–456.
7. Lawton, L. A.; Edwards, C.; Codd, G. A. Extraction and High-Performance Liquid Chromatographic Method for the Determination of Microcystins in Raw and Treated Waters. *Analyst* **1994**, *119* (7), 1525–1530.
8. Gago-Martínez, A.; Piñeiro, N.; Aguete, E. C.; Vaquero, E.; Nogueiras, M.; Leão, J. M.; Rodríguez-Vázquez, J. A.; Dabek-Zlotorzynska, E. Further Improvements in the Application of High-Performance Liquid Chromatography, Capillary Electrophoresis and Capillary Electrochromatography to the Analysis of Algal Toxins in the Aquatic Environment. *J. Chromatogr. A* **2003**, *992* (1–2), 159–168.
9. Zhang, L. F.; Ping, X. F.; Yang, Z. G. Determination of Microcystin-LR in Surface Water Using High-Performance Liquid Chromatography/Tandem Electrospray Ionization Mass Detector. *Talanta* **2004**, *62*, 193–200.
10. Cong, L. M.; Huang B. F.; Chen, Q.; Lu, B. Y.; Zhang, J.; Ren, Y. P. Determination of Trace Amount of Microcystins in Water Samples Using Liquid Chromatography Coupled with Triple Quadrupole Mass Spectrometry. *Anal. Chimi. Acta* **2006**, *569*, 157–168.
11. Mekebri, A.; Blondina, G. J.; Crane, D. B. Method Validation of Microcystins in Water and Tissue by Enhanced Liquid Chromatography Tandem Mass Spectrometry. *J. Chromatogr. A* **2009**, *1216*, 3147–3155.

12. ISO 20179: 2005. Water Quality-Determination of Microcystins-Method Using Solid Phase Extraction (SPE) and High Performance Liquid Chromatography (HPLC) with Ultraviolet (UV) Detection, International Standardization Organization, Switzerland.
13. Lee, H. S.; Jeong, C. K.; Lee, H. M.; Choi, S. J.; Do, K, S.; Kim, K.; Kim, Y. H. On-Line Trace Enrichment for the Simultaneous Determination of Microcystins in Aqueous Samples Using High-Performance Liquid Chromatography with Diode-Array Detection. *J. Chromatogr. A* **1999**, *848*, 179–184.
14. Ramanan, S.; Tang J.; Velayudhan, A. Isolation and Preparative Purification of Microcystin Variants. *J. Chromatogr. A* **2000**, *883*, 103–112.
15. Ammerman, J. L.; Aldstadt III, J. H. Monolithic Solid-Phase Extraction for the Rapid on-Line Monitoring of Microcystins in Surface Waters. *Microchim. Acta* **2009**, *164*, 185–196.
16. Spoof, L.; Meriluoto, J. Rapid Separation of Microcystins and Nodularin Using a Monolithic Silica C_{18} Column. *J. Chromatogr. A* **2002**, *947*, 237–245.
17. Zhao, Y. Y.; Hrudey, S.; Li, X. F. Determination of Microcystins in Water Using Integrated Solid-Phase Microextraction with Microbore High-Performance Liquid Chromatography–Electrospray Quadruple Time-of-Flight Mass Spectrometry, *J. Chromatogr. Sci.* **2006**, *44*, 359–365.
18. Pavagadhi, S.; Basheer, C.; Balasubramanian, R. Application of Ionic-Liquid Supported Cloud Point Extraction for the Determination of Microcystin-leucine–arginine in Natural Waters. *Anal. Chimi. Acta* **2011**, *686*, 87–92.
19. Man, B. K. W.; Lam, M. H. W.; Lam, P. S.; Wu R. S. S.; Shaw, G. Cloud-Point Extraction and Preconcentration of Cyanobacterial Toxins (Microcystins) from Natural Waters Using a Cationic Surfactant. *Environ. Sci. Technol*. **2002**, *36* (18), 3985–3990.
20. GB/T 20466-2006. Determination of Microcystins in Water. Standardization Administration of the People's Republic of China, China.
21. Ma, J. P.; Xiao, R. H.; Li, J. H.; Yu, J. B.; Zhang, Y. Q.; Chen, L. X. Determination of 16 Polycyclic Aromatic Hydrocarbons in Environmental Water Samples by Solid-Phase Extraction Using Multi-Walled Carbon Nanotubes as Adsorbent Coupled with Gas Chromatography–Mass Spectrometry. *J. Chromatogr. A* **2010**, *1217* (34), 5462–5469.
22. Ma, J. P.; Xiao, R. H.; Li, J. H.; Li, J.; Shi, B. Z.; Liang, Y. J.; Lu, W. H.; Chen, L. X. Headspace Solid-Phase Microextraction with on-Fiber Derivatization for the Determination of Aldehydes in Algae by Gas Chromatography–Mass Spectrometry. *J. Sep. Sci.* **2011**, *34* (12), 1477–1483.
23. Alpendurada, M. D. Solid-Phase Microextraction: A Promising Technique for Sample Preparation in Environmental Analysis. *J. Chromatogr. A* **2000**, *889*, 3–14.
24. Song, Y. R.; Zhao, S. L.; Tchounwou, P.; Liu, Y. M. A Nanoparticle-Based Solid-Phase Extraction Method for Liquid Chromatography–Electrospray Ionization-Tandem Mass Spectrometric Analysis. *J. Chromatogr. A* **2007**, *1166* (1–2), 79–84.
25. Liu, Y.; Li, H. F.; Lin J. M. Magnetic Solid-Phase Extraction Based on Octadecyl Functionalization of Monodisperse Magnetic Ferrite Microspheres for the Determination of Polycyclic Aromatic Hydrocarbons in Aqueous Samples Coupled with Gas Chromatography-Mass Spectrometry. *Talanta* **2009**, *77* (3), 1037–1042.
26. Li, J. D.; Zhao, X. L.; Shi, Y. L.; Cai, Y. Q. Mixed Hemimicelles Solid-Phase Extraction Based on Etyltrimethylammonium Bromide-Coated Nano-Magnets Fe_3O_4 for the Determination of Chlorophenols in Environmental Water Samples Coupled with Liquid Chromatography/Spectrophotometry Detection. *J. Chromatogr. A* **2008**, *1180* (1–2), 24–31.
27. Han, Q.; Wang, Z. H.; Xia, J. F. Facile and Tunable Fabrication of Fe_3O_4/Graphene Oxide Nanocomposites and Their Application in the Magnetic Solid-Phase Extraction of Polycyclic Aromatic Hydrocarbons from Environmental Water Samples. *Talanta* **2012**, *101*, 388–395.
28. Zhao, G. Y.; Song, S. J.; Wang, C. Determination of Triazine Herbicides in Environmental Water Samples by High-Performance Liquid Chromatography Using Graphene-Coated Magnetic Nanoparticles as Adsorbent. *Anal. Chim. Acta* **2011**, *78* (1–2), 155–159.
29. Zhang, Z.; Li, J. H.; Fu, J. Q.; Chen, L. X. Fluorescent and Magnetic Dual-Responsive Coreshell Imprinting Microspheres Strategy for Recognition and Detection of Phycocyanin. *RSC Adv*. **2014**, *4*, 20677–20685.
30. Yu, P. F.; Wang, Q.; Zhang, X. F.; Zhang, X. S.; Shen, S.; Wang, Y. Development of Superparamagnetic High-Magnetization C_{18}-Functionalized Magnetic Silica Nanoparticles as Sorbents for Enrichment and Determination of Methylprednisolone in Rat Plasma by High Performance Liquid Chromatography. *Anal. Chim. Acta* **2010**, *678* (1), 50–55.
31. Sha, Y. F.; Deng, C. H.; Liu, B. Z. Development of C_{18}-Functionalized Magnetic Silica Nanoparticles as Sample Preparation Technique for the Determination of Ergosterol in Cigarettes by Microwave-Assisted Derivatization and Gas Chromatography/Mass Spectrometry. *J. Chromatogr. A* **2008**, 1198–1199, 27–33.
32. Maddah, B.; Shamsi, J. Extraction and Preconcentration of Trace Amounts of Diazinon and Fenitrothion from Environmental Water by Magnetite Octadecylsilane Nanoparticles. *J. Chromatogr. A* **2012**, *1256*, 40–45.
33. Chen, X. G.; Xiao, B. D.; Ao, H. Y.; Chen, X. D.; Xu, X. Q. Relationship between Retention on Chromatography and Charge State of Microcystins. *J. Wuhan Univ. Technol*. **2005**, *27*, 19–21.
34. Ballesteros-Gómez, A.; Rubio, S. Hemimicelles of Alkyl Carboxylates Chemisorbed onto Magnetic Nanoparticles: Study and Application to the Extraction of Carcinogenic Polycyclic Aromatic Hydrocarbons in Environmental Water Samples. *Anal. Chem*. **2009**, *81*, 9012–9020.

ISSN 1615-9306 · JSSCCJ 38 (20) 3487–3668 (2015) · Vol. 38 · No. 20 · October 2015 · D 10609

JSS

JOURNAL OF

SEPARATION SCIENCE

20|15

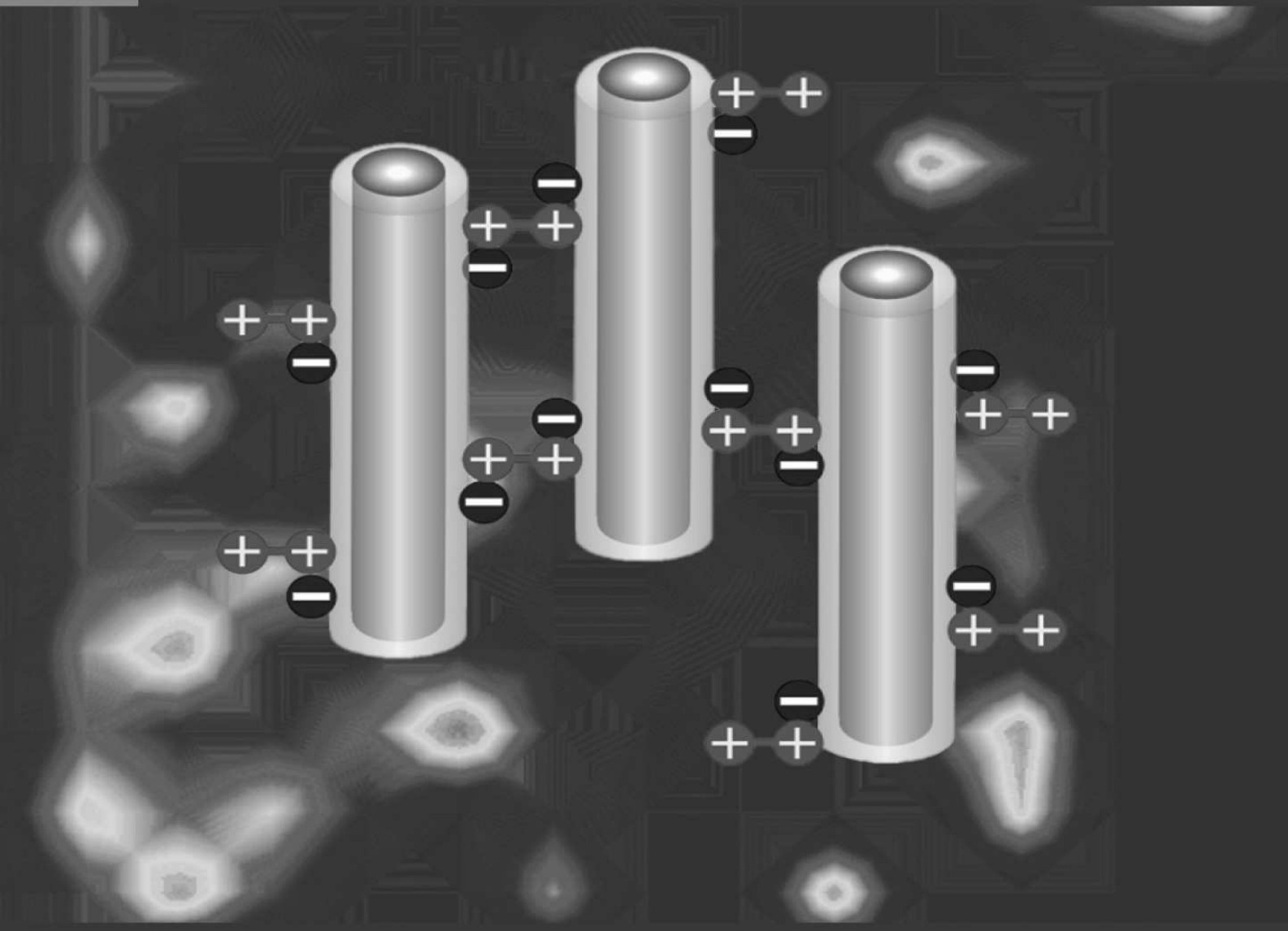

Methods

Chromatography · Electroseparation

Applications

Biomedicine · Foods · Environment

www.jss-journal.com

WILEY

Charalampos S. Binellas
Constantine D. Stalikas

Department of Chemistry, University of Ioannina, Ioannina, Greece

Received May 14, 2015
Revised July 7, 2015
Accepted July 29, 2015

Research Article

Magnetic octadecyl-based matrix solid-phase dispersion coupled with gas chromatography with mass spectrometry in a proof-of-concept determination of multi-class pesticide residues in carrots

A novel procedure is put forward based on the combination of the well-established matrix solid-phase dispersion and the magnetic and sorption properties of magnetic octadecyl in the presence of *n*-octanol and was employed in a proof-of-concept sample preparation and determination of several classes of pesticide residues in carrots. The procedure does not require the transfer of blend to cartridge and subsequent packing, nor any co-sorbent for extract clean up. The hydrophobic magnetic nanoparticles utilized as a sorbent, can be retrieved by *n*-octanol under the application of a magnetic field due to hydrophobic interactions. Elution of pesticide residues is then carried out with an organic solvent. A total of 26 pesticides were included in this procedure and the target compounds were analyzed using gas chromatography with mass spectrometry in the selective ion monitoring mode. The average extraction recoveries obtained from carrot samples fortified at three different concentrations (20, 50, and 500 μg/kg) were 77–107%. The estimated limits of quantitation for most target analytes were in the low μg/kg level. The study demonstrates that the proposed extraction procedure is simple and effective, avoiding a clean-up step for the sample preparation of vegetable.

Keywords: Carrots / Gas chromatography with mass spectrometry / Magnetic octadecyl nanosorbent / Matrix solid-phase dispersion / Pesticide residues
DOI 10.1002/jssc.201500519

Additional supporting information may be found in the online version of this article at the publisher's web-site

1 Introduction

Pesticides may pose different toxicities to human health, depending on their chemical class. For this reason, pesticide residue analysis in food is one of the most important and challenging tasks in routine laboratory practice. In this context, the European legislation (European Regulation 396/2005) sets maximum residue limits (MRLs) of pesticide residues in different products of plant and animal origin [1]. The regulation issues a default limit of 0.01 mg/kg for all pesticide / commodity combinations for which no MRLs have been set, unless MRLs are not required or different defaults have been set. To comply with these strict regulations and directives organizations are heavily investing into in-depth research to identify the most efficient method for pesticide residue analysis in food. Therefore, a significant analytical challenge should be met with respect to the LODs and LOQs required for some specified food matrices.

Separation and quantification of thermally stable pesticides is mainly carried out by GC–MS, since it allows the simultaneous determination of several compounds belonging to different classes [2]. As regards sample preparation, SPE [3, 4], SPME, stir bar sorptive extraction [5], microporous membrane LLE [6], PLE [7], dispersive liquid–liquid microextraction [8–10], and QuEChERS [9, 10] are some of the many sample preparation techniques used for the extraction of pesticides and sample cleanup. Matrix solid-phase dispersion (MSPD) is also employed for the determination of pesticide residues in foodstuff [11] since it offers an excellent alternative to conventional sample preparation techniques. Although MSPD was initially intended to be used with biological samples, further studies have demonstrated its usefulness for the extraction of organic compounds and especially pesticides from solid matrices such as dried soil [12, 13]. It combines the sampling, extraction and cleanup into a single step, which eliminates the complications of LLE and SPE

Correspondence: Prof. Constantine D. Stalikas, Department of Chemistry, University of Ioannina, Ioannina 45110, Greece
E-mail: cstalika@cc.uoi.gr
Fax: +30 26510 08796

Abbreviations: MSPD, matrix solid-phase dispersion; **MRL**, maximum residue limit; **SIM**, selective ion monitoring

for solid and semi-solid samples. For these reasons it has found particular application as an analytical process for the preparation, extraction, and fractionation of solid, semi-solid, and/or highly viscous biological samples. In the MSPD process, a sample is placed in a glass or agate mortar containing the appropriate sorbent or other support material wherein they are manually blended together using a glass or agate pestle. Also, internal standards or spikes may be added before this step. The blended material is then transferred and packed into a column suitable for conducting sequential elution with solvents [14]. The most commonly materials used in MSPD are reversed-phase and normal-phase sorbents, like octadecylsilane (C_{18}) [15,16], octyl-bonded silica [17,18], silica gel [19], NH_2-silica [20], and polymeric sorbents [21,22]. Recently, molecularly imprinted polymers [21,22] and multiwall carbon nanotubes have been used [23]. The key characteristics of MSPD are its versatility, high throughput, low cost, and rapidity.

Magnetic nanoparticles are widely used in detection and analytical systems because of their performance advantages compared to solids that lack magnetic properties. Magnetic solid separation techniques also offer benefits over centrifugation, filtration and classical SPE [24,25]. Depending on their functionalization, they can be used for the preconcentration of analytes from liquid samples and the magnetic separation and molecular identification of biomolecules, organic and inorganic species. Up until now, magnetic nanomaterials properly modified with organic moieties have been used for the sample preparation of solid matrices after they have first been extracted with an organic solvent [26–31]. Also, magnetic nanoparticles have been successfully employed in combination with graphitized carbon black for purification purposes using a modified QuEChERS method [32].

In this study, we propose for the first time, a procedure based on the combination of the principles of MSPD with the magnetic and sorption properties of iron oxide-C_{18}, in the presence of *n*-octanol, for sample preparation and multi-class pesticide residues determination in vegetables. A proof-of-principle work was applied to pesticide residues in carrot demonstrating the feasibility of the concept. The procedure does not require the transfer of blend into cartridge and subsequent packing, nor any co-sorbent for extract clean up. The *n*-octanol employed assists in blending the mixture and most importantly, in detaching the nanosorbent from the vegetable matrix, in the aqueous phase, where the sample matrix is then transferred. The separation of the analytes and their quantitation are performed by GC–MS. Overall, the resulting method is proved to be efficient and straightforward for the particular purpose.

2 Materials and methods

2.1 Chemicals and reagents

All the chemical and reagents used were of analytical grade. Anhydrous ferric chloride and ferrous chloride tetrahydrate were from Merck (Darmstadt, Germany) and Sigma–Aldrich (Sigma–Aldrich Hellas, Greece), respectively. Tetraethyl orthosilicate (TEOS) and trimethoxy(octadecyl)silane (99%) were purchased from Aldrich and Riedel-de-Haen (Seelze-Hannover, Germany). The pesticides studied were obtained from Riedel-de-Haen and Aldrich, acetone and ethyl acetate from Fisher Chemicals (Loughborough, UK), *n*-octanol from Scharlau (Barcelona, Spain), and ammonia from Sigma–Aldrich.

Individual stock standard solutions of the pesticides studied were prepared at a concentration of 1000 μg/mL in acetone, by exact weighing of high-purity substances and were stored at −18°C, in the dark. Then, a mixture of all the compounds was prepared in acetone containing 5 μg/mL of each individual pesticide.

2.2 Instrumentation and chromatographic conditions

A Shimadzu GC–17A gas chromatograph (Kyoto, Japan), interfaced with a Shimadzu QP 5000 mass spectrometer was equipped with a split/splitless injector and a DB5-MS column (30 m × 0.25 mm i.d., 0.25 μm film thickness, Agilent J&W, Agilent Technologies, CA, USA) for the separation of the analytes. The injector and mass transfer-line temperatures were set at 250 and 290°C, respectively. Injections were performed using an angle-cut needle tip (0.6 mm glass barrel, i.d.; 0.11 mm needle i.d.) purchased from Hamilton (Reno, Nevada, USA).

The column temperature was programmed at 50°C for 1 min, increased to 150°C, at a rate of 15°C/min, then to 260°C, at a rate of 4°C/min and held for 10 min. The total run time was 45.17 min. The mass detector was operated in the electron impact mode, at 70 eV with the electron multiplier voltage set to 1.34 kV. The solvent cut time was 6.0 min. The injection volume was 1.0 μL and splitless injection mode was employed. The splitless time was 1.0 min. Helium (purity ≥ 99.999%) was used as the carrier gas, at a flow rate of 1.0 mL/min. Selective ion monitoring (SIM) mode was adopted for qualification and quantification of the analytes of concern (see Table 1).

2.3 Synthesis of nanometer-sized C_{18}-silica magnetic particles (Fe_3O_4@SiO_2@C_{18})

The synthesis of the silica modified magnetic nanoparticles was based on our previously described procedure [33]. Briefly, tetrahydrate iron (III) chloride and hexahydrate iron (II) chloride were mixed together in double distilled water, where 25% ammonia was also added to form a black precipitate of iron oxide particles. The suspension was heated and stirred for 30 min and after being washed several times with water and ethanol, the iron oxide powder was dried at 70°C. Subsequently, the nanoparticles were coated with tetraethoxysilane in ammoniac ethanol under stirring and nitrogen atmosphere, overnight. The dried silica-coated nanoparticles

Table 1. Parameters of pesticides determined by GC-MS (SIM). Determination coefficients (R^2), LODs, and LOQs for the matrix-matched curves of the pesticides

Compound	Compound class	t_R (min)	Ions (*m/z*)	Determination coefficient (R^2)	LOD[a] (μg/kg)	LOQ[b] (μg/kg)
Carbofuran	Carbamate	10.1	131, 149, 164	0.9982	4.5	14
Butylate	Thiocarbamate	12.1	146, 156, 174	0.9980	4.5	14
Propachlor	Chloroacetanilide	15.6	77, 120, 176	0.9963	4.0	12
Ethoprophos	Organophosphorus	16.1	97, 139, 158	0.9996	6.0	18
Trifluralin	Nitroaniline	16.7	264, 290, 306	0.9961	12.5	37
Cadusafos	Triazine	17.3	97, 127, 159	0.9983	8.5	25
Atrazine	Triazine	18.7	173, 200, 215	0.9984	4.0	12
Cyromazine	Benzamide	19.3	109, 151, 166	0.9965	6.0	18
Propyzamide	Pyrethroid	19.6	145, 175, 255	0.9988	12.5	37
Tefluthrin	Organochloride	20.2	141, 177, 197	0.9974	8.5	25
Endosulfan ether	Organochloride	21.4	69, 241, 277	0.9981	4.0	12
Vinclosolin	Dicarboximide	22.1	198, 212, 285	0.9965	6.0	18
Parathion methyl	Organophosphorus	22.3	109, 125, 263	0.9988	12.5	37
Fenchlorphos	Organothiophosphate	22.7	109, 125	0.9970	8.5	25
Bromophos methyl	Dimethylchlorthiophosphate	25.2	109, 125, 331	0.9953	4.0	12
Penconazole	Triazole	26.1	159, 248	0.9973	8.5	25
Procymidone	Dicarboximide	26.7	93, 283	0.9949	20	6
Triadimenol	Triazole	27.0	112, 128, 168	0.9976	34	102
Methidathion	I.S.	27.2	85, 112, 145			
Fenamiphos	Organophosphorus	28.2	154, 217, 303	0.9972	20.5	61
Kresoxim methyl	Strobilurin analogue	29.3	116, 131, 206,	0.9977	4.5	13
Fluazifop-p-butyl	Aryloxyphenoxypropionates	30.0	125, 222	0.9975	3.0	9
Ofurace	Phenylamide	31.9	132, 160, 232,	0.9949	32	96
Bifenthrin	Pyrethroid	34.9	165, 181	0.9948	1.0	3
Fenoxycarb	Carbamate	35.2	116, 186, 255	0.9973	24	72
Pyriproxyfen	Pyridine-based	37.2	136, 226	0.9974	3.0	9
Biternanol	Azole	40.4	112, 170	0.9950	46	137

a) LOQ: limit of quantitation, defined as the lowest concentration that can be quantified with acceptable recovery (70–120%) and precision (RSD < 20%).
b) LOD: limit of detection, et at 1/3 LOQ.

were dispersed in toluene and trimethoxy(octadecyl)silane was added, under vigorous stirring, once the slurry was brought to boiling. The mixture was refluxed for 12 h and after cooling down, the black-brown product was washed several times with toluene and ethanol and dried at 70°C.

2.4 Samples and sample preparation

Carrot samples used for the development of the procedure were purchased from local supermarkets. A representative portion of the root vegetable (~200 g of carrot) was chopped with a stainless-steel knife, homogenized using a household blender and dried in an oven, overnight, at 70°C. Spiking procedure consisted of adding aliquots of the stock standard solution to 2 g of carrot, soaked in acetone. The mixtures were dried under vacuum, at room temperature to let pesticides penetrate into the matrix and then closed and stored in the freezer at −18°C, for at least one week before extraction.

The concentrations of pesticides in the resulting spiked samples were checked by the developed optimized method and were found to be from 3 to 1200 μg/kg.

2.5 Magnetic C_{18}-based matrix solid-phase dispersion procedure

An aliquot of 200 mg of the root vegetable sample was placed into an agate mortar, where it was strongly blended with 60 mg of magnetic sorbent by way of a pestle, for 2 min, to achieve disruption of the sample matrix and full dispersion of the nanosorbent. Afterward, 200 μL of *n*-octanol was added in the homogeneous, dark-colored mixture followed by a gentle blending, for 1 min. The sample was transferred quantitatively with 100 mL of double distilled water into a glass beaker along with the washings of the mortar and pestle, followed by ultrasonication for 3 min. During this procedure, the magnetic nanoparticles aggregated into *n*-octanol drops, which were floating on the surface of the aqueous phase. In this way, the vegetable particles were left bare at the bottom of the glass beaker while the sorbent along with the organic solvent were harvested by placing an ordinary magnet at the side of the beaker and were removed easily after pouring (See photos in the Supporting Information). Subsequently, traces of water were evaporated by blowing a gentle nitrogen stream for 5 min and the pesticides were eluted with 3 mL of ethyl acetate by applying ultrasonication, for 2 min. The eluates were

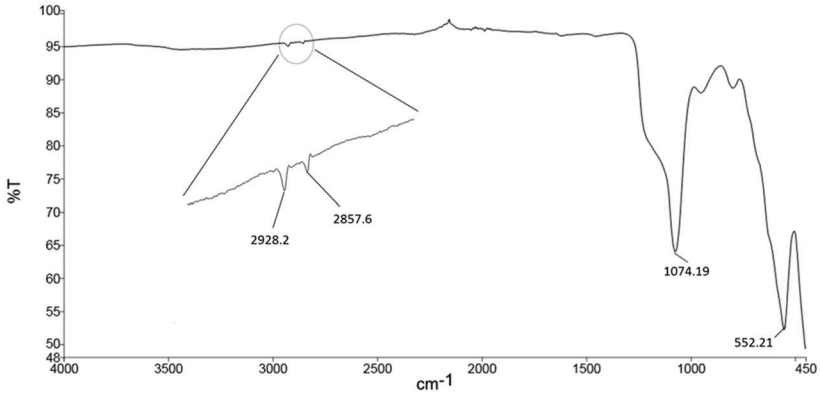

Figure 1. FTIR spectrum of $Fe_3O_4@SiO_2@C_{18}$. The peaks at 2928 and 2857 cm^{-1} in the inset, reveal the presence of $(CH_2)_{17}CH_3$. The peaks at 1074 and 552 cm^{-1} reveal the presence of Si–O–Si and Fe–O–Fe, respectively.

separated from the magnetic nanoparticles by a magnet and collected in a different vial. The solution was concentrated to 250 μL under a gentle nitrogen steam, after the addition of the methidathion, as internal standard (I.S.) and 1 μL of the final extract was directly analyzed by GC–MS.

3 Results and discussion

3.1 Characterization of the sorbent

The characterization of the synthesized nanosorbent at the different steps of synthesis (iron oxide, magnetic silica, and magnetic silica-C_{18}) was carried out as described in our previous publication [24]. The elemental analysis of the nanosorbent showed a carbon content of 7.3%. The FTIR spectrum (Fig. 1), received by an attenuated total reflectance accessory (PerkinElmer, MA, USA) revealed the presence of the stretching vibration Fe—O—Fe at 552 cm^{-1}, the Si—O—Si vibration at 1074 cm^{-1} and the asymmetric and the symmetric extension vibration of CH_2 in the $(CH_2)_{17}CH_3$ at 2928 and 2857 cm^{-1}, respectively.

3.2 Optimization of the proposed procedure

The univariate optimization of the MSPD procedure for the extraction of several classes of pesticide residues comprised the following: amount of the sorbent, matrix dispersion solvent, presence of salt, and polarity of the elution solvent. For the optimization, 200 mg of dried, pesticide-free carrot, fortified at 500 μg/kg level, were extracted and analyzed. To evaluate the influence of the above mentioned parameters, the total area of the chromatographic peaks corresponding to the studied pesticide residues was considered. It should be mentioned that the vegetable matrices should have been dried before blending. The presence of considerable amount of water causes the nanosorbent to be dispersed unevenly in the matrix due to its highly hydrophobic character and the low dimensions of particles, with concomitant low recoveries of the analytes. At lower water content, the recoveries were significantly improved approaching the recovery figures of

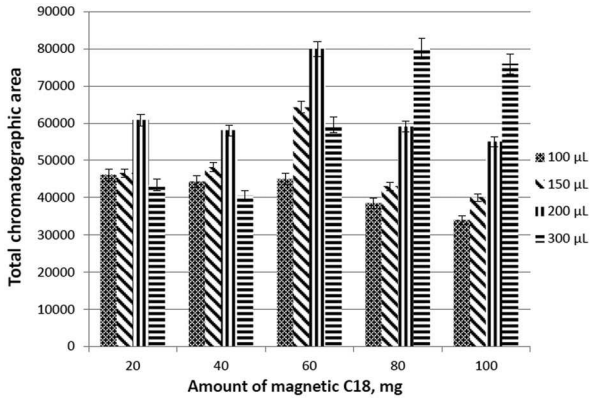

Figure 2. Effect of the amount of magnetic C_{18} at different volumes of *n*-octanol on the total chromatographic peak area of pesticides.

the process in dried sample. Since water content varies from matrix to matrix, we opted for a drying step before extraction rather than choosing a matrix with lower content of water.

Initially, the role of solvent in the procedure during the blending step was tested. The *n*-octanol is a solvent with density lower than water, relatively less toxic than other organic solvents and magnetic nanoparticles can retrieve in it from aqueous solution, by hydrophobic interactions. Apart from *n*-octanol, other water-immiscible organic solvents like ethyl acetate, *n*-butanol and *n*-hexane were chosen. The extraction yield was proved to be the highest with *n*-octanol as compared to the recoveries of pesticides with the remainder of the tested solvents. The situation was the worst with the least polar *n*-hexane, which was proven to be hardly manipulated, when in contact with water, after the blending step.

The amount of sorbent, in the presence of *n*-octanol was studied, at different ratios of vegetable matrix-to-sorbent and sorbent-to-octanol. That is to say, 200 mg of vegetable were treated with 20, 40, 60, 80, and 100 mg of magnetic-C_{18} in the presence of 100, 150, 200, and 300 μL of *n*-octanol. As can be seen in Fig. 2, generally, the recovery rose with an increase in the amount of sorbent from 20 to 60 mg and then the behavior becomes rather inexplicable. Apparently, the volume of *n*-octanol and the amount of sorbent are interrelated

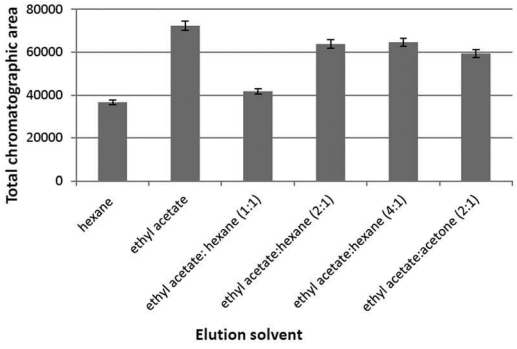

Figure 3. Effect of different solvents on the elution of pesticide residues form the magnetic C_{18}.

and therefore, the effectiveness of the MSPD procedure depends on the sorbent/solvent combination. High amounts of sorbent in combination with low volumes of *n*-octanol, during MSPD (e.g. 100 mg with 100 μL of *n*-octanol), resulted in low chromatographic peaks and higher variability of the results due to incomplete isolation of the magnetic sorbent. That was also the case with small amounts of sorbent with increased volumes of *n*-octanol (e.g. 20 mg sorbent with 300 μL of *n*-octanol). As the role of *n*-octanol is mainly to assist the blending and isolate the nanosorbent form the vegetable matrix and aqueous phase at a next stage (see discussion below, in this sub-section), low volumes were insufficient to accomplish this task. On the other hand, when *n*-octanol is in excess in relation to the sorbent mass, its greater dispersibility within the bulk aqueous phase in the glass beaker renders the collection of magnetic nanosorbent cumbersome. For the above reasons and considering the difficulties in concentrating of *n*-octanol after elution, 60 mg of the sorbent and 200 μL of *n*-octanol were a compromise to extract efficiently the pesticide residues from 200 mg of dried vegetables.

Additional experiments were undertaken to evaluate the efficiency of the elution solvent after the collection of the magnetic nanosorbent, which had already been dispersed in *n*-octanol. Using the optimized proportions, i.e. 200 mg of sample, 60 mg of magnetic C_{18} and 200 μL of *n*-octanol, the ethyl acetate, *n*-hexane, methyl-*tert*-butyl ether and the mixtures ethyl acetate/acetone (2:1 v/v), and ethyl acetate/*n*-hexane (1:1, 2:1, 4:1, v/v) were tested as eluents, for the pesticide residues from the sorbent. The results depicted in Fig. 3, showed that the elution strength of ethyl acetate was higher than that of the rest of the solvents. Subsequently, the volume of the eluent was tested by using ethyl acetate volume increments of 2.0, 3.0, and 4.0 mL. A final volume of 3.0 mL was enough to elute quantitatively the pesticide residues from the magnetic nanosorbent.

The need for ultrasonication in several steps of the procedure was also studied. After the sample has been transferred into a glass beaker, ultrasonication was applied for 3 min to help the matrix compounds separate from the sorbent, in the presence of the *n*-octanol drops. Omitting this step is the primary reason for the requirement of longer time to separate nanomaterial from the bulk sample. In addition, a 2 min ultrasonication step was also mandatory in the elution step to effectively elute the analytes from the magnetic nanoparticles.

Finally, the effect of the presence of salt in the procedure was examined. To this end, NaCl, Na_2SO_4, and $MgSO_4$ were utilized during the blending step, in three different quantities i.e. 200, 500, and 1000 mg, each. In any case, the addition of salt did not provoke any effect as the obtained recoveries showed results similar to those in the absence of salts. These salts are commonly used as drying agents in MSPD procedures. As the samples used to apply the procedure were previously dried, the presence of any of these salts would not be necessary for the particular purpose. Moreover, the presence of salt does not serve the purpose of easier phase separation nor does it cause any salting out effect in a subsequent step of isolation of pesticide-loaded magnetic nanosorbent. Therefore, all the experiments were carried out without adding any salt.

3.3 Validation of the multiresidue analytical procedure

The analytical method developed, which relied on the principles of the proposed magnetic C_{18}-based MSPD procedure was validated in terms of linearity, accuracy, precision, and limits of quantitation of the target analytes based on the SANCO/12571/2013 European Guidelines [34]. The specificity of the proposed MSPD procedure was assessed by the analysis of blank samples. The MSPD extracts are clean enough to be directly subjected to instrumental analysis with no need for cleanup steps. The absence of chromatographic peaks at the retention times where the target analytes were eluted indicated that there were no matrix interferences that might give a false positive or negative signal. To reconcile differences in sample matrices of vegetables, calibration curves were calculated with a matrix-matched standard calibration in blank samples (see Supporting Information Figs. S1 and S2 for representative GC–MS(SIM) chromatograms of non-spiked and spiked sample). More specifically, the working linear ranges for all the pesticides were determined using blank samples fortified with known amounts of the analytes, which ranged from 3 μg/kg (bifenthrin) to 1200 μg/kg (biternanol). The resulting calibration curves (seven points of analyte-to-I.S. areas, each calibration point in triplicate) gave a high level of linearity for all target analytes with coefficients of determination (R^2) ranging between 0.9949 and 0.9997 while most of the LODs were below 10 μg/kg (Table 1).

The accuracy and precision of the developed method were determined by spiking uncontaminated carrot samples, at three different concentration levels (i.e. 20, 50, and 500 μg/kg). Accuracy is expressed as analyte recovery i.e. percent closeness between the calculated and the theoretical concentrations of the spiked carrot samples for each analyte. The within-day repeatability and between-day reproducibility were calculated as the RSD% of five and three replicates (i.e. three consecutive days), respectively. As shown in Table 2,

Table 2. Recovery and relative standard deviation (RSD) values obtained with the magnetic C_{18}-based MPSD procedure, at three concentration levels, in carrot

Compound	Fortification level at 20 μg/kg			Fortification level at 50 μg/kg			Fortification level at 500 μg/kg		
	Recovery* (%)	Within-day RSD (%)	Between-day RSD (%)	Recovery (%)	Within-day RSD (%)	Between-day RSD (%)	Recovery (%)	Within-day RSD (%)	Between-day RSD (%)
Carbofuran	90	6.3	7.9	89	6.8	9.5	92	6.0	8.7
Butylate	95	2.6	4.0	105	1.2	4.1	85	4.1	3.8
Propachlor	93	5.1	6.3	82	7.6	8.9	103	8.9	9.8
Ethoprophos	80	3.9	4.5	78	3.7	3.2	77	5.4	9.1
Trifluralin	-	-	-	84	5.0	4.9	106	7.8	9.6
Cadusafos	-	-	-	91	5.8	7.5	81	8.2	8.9
Atrazine	91	3.5	5.7	88	1.4	2.6	86	4.6	7.8
Cyromazine	97	7.6	8.1	96	7.1	6.4	102	9.8	8.9
Propyzamide	-	-	-	99	2.9	9.7	105	1.9	8.9
Tefluthrin	-	-	-	92	1.3	5.4	97	1.3	3.3
Endosulfan ether	93	3.8	5.1	96	4.9	3.9	95	2.3	5.1
Vinclosolin	89	6.1	6.9	88	5.9	6.5	94	8.7	8.0
Parathion methyl	-	-	-	97	7.9	6.8	83	8.2	9.7
Fenchlorphos	-	-	-	86	5.0	5.6	103	1.4	5.9
Bromophos methyl	98	6.9	8.6	107	9.1	7.1	96	5.3	10.1
Penconazole	-	-	-	94	1.9	6.0	77	4.7	8.2
Procymidone	95	4.4	5.9	96	5.5	10.1	92	3.6	6.0
Triadimenol	-	-	-	-	-	-	86	8.1	8.0
Fenamiphos	-	-	-	-	-	-	87	6.1	6.0
Kresoxim methyl	92	4.8	8.1	99	5.0	9.1	85	3.7	8.5
Fluazifop-p-butyl	95	5.1	6.4	91	6.8	4.4	101	2.6	6.9
Ofurace	-	-	-	-	-	-	81	5.4	6.7
Bifenthrin	86	5.8	7.1	79	5.4	6.3	88	5.4	9.8
Fenoxycarb	-	-	-	-	-	-	99	2.9	5.5
Pyriproxifen	89	6.7	8.4	95	8.7	8.1	84	6.3	7.4
Biternanol	-	-	-	-	-	-	92	9.7	9.1

*Recovery and RSD values are not reported when the spiking level is lower than the LOQ of the respective analyte.

recovery values between 77 and 107% were obtained, with RSDs up to 10.1%, all of them being within the acceptable range for routine analyses.

The reusability of the magnetic material was not contemplated because tiny pieces of carrot attach to the magnetic particles rendering them unsuitable for further use. The developed magnetic-based matrix solid-phase dispersion was applied to the determination of pesticide residues in carrot samples. Three different samples were analyzed. No pesticide residues were found at concentrations above the detection limits of the method.

4 Concluding remarks

Magnetic-C_{18} has been established in the analytical research field as a successful and promising material for sample treatment due to ease of preparation, efficiency and simple removal. In the present study, a novel procedure was developed by expanding on the notion of MSPD and C_{18} sorption-magnetic separation, in the presence of *n*-octanol and investigating the proof of concept of determining pesticide residues in a vegetable. The hydrophobic magnetic nanomaterial was utilized as sorbent, which can be retrieved in *n*-octanol as a result of hydrophobic interactions and they can be separated under the application of a magnetic field. The study demonstrates that the pretreatment technique is simple and effective, avoiding clean-up steps for the sample preparation of carrot before the determination of pesticide residues. In addition, the developed procedure provides satisfactory accuracy and precision. Work is underway to test other less hydrophobic magnetic sorbents, which may take advantage of other interactions to widen applicability of the concept and make it more compatible with high-water-content matrices.

The authors have declared no conflict of interest.

5 References

[1] EC, 2005. Regulation (EC) No 396/2005 of the European Parliament and of the Council of 23 February 2005 on maximum residue levels of pesticides in or on food and feed of plant and animal origin and amending Council Directive 91/414/EEC. Official J. L 70, 16.3.2005, 1–16.

[2] Karamani, A. A., Fiamegos, Y. C., Vartholomatos, G., Stalikas, C. D., *J. Chromatogr. A* 2013, *1302*, 125–132.

[3] Schenck, F. J., Lehotay, S. J., Vega, V., *J. Sep. Sci.* 2002, *25*, 883–890.

[4] Albero, B., Sanchez-Brunete, C., Tadeo, J. L., *Talanta* 2005, *66*, 917–924.

[5] Ochiai, N., Sasamoto, K., Kanda, H., Yamagami, T., David, F., Tienpont, B., Sandra, P., *J. Sep. Sci.* 2005, *28*, 1083–1092.

[6] Hyötyläinen, T., Tuutijärvi, T., Kuosmanen, K., Riekkola, M.-L., *Anal. Bioanal. Chem.* 2002, *372*, 732–736.

[7] Garrido Frenich, A., Martínez Salvador, I., Martínez Vidal, J. L., López-López, T., *Anal. Bioanal. Chem.* 2005, *3*, 1106–1118.

[8] Farajzadeh, M. A., Khoshmaram, L., Nabil, A. A. A., *J. Food Comp. Anal.* 2014, *34*, 128–135.

[9] Silva, V. D., Simão, V., Dias, A. N., Carletto, J. S., Carasek, E., *J. Sep. Sci.* 2015, *38*, 1959–1968.

[10] He, Z., Wang, L., Peng, Y., Luo, M., Wang, W., Liu, X., *Food Chem.* 2015, *169*, 372–380.

[11] Wen, Y., Chen, L., Li, J., Liu, D., Chen, L., *TrAC Trends Anal. Chem.* 2014, *59*, 26–41.

[12] Carpinteiro, I., Casado, J., Rodríguez, I., Ramil, M., Cela, R., *J. Sep. Sci.* 2012, *35*, 853–860.

[13] Wang, H., Yan, H., Qiao, J., *J. Sep. Sci.* 2012, *35*, 292–298.

[14] Barker, S. A., *J. Biochem. Biophys. Methods* 2007, *70*, 151–162.

[15] Soler, C., Mañes, J., Picó, Y., *J. Chromatogr. A* 2004, *1048*, 41–49.

[16] Rodrigues, S. A., Caldas, S. S., Primel, E. G., *Anal. Chim. Acta* 2010, *678*, 82–89.

[17] Valenzuela, A. I., Lorenzini, R., Redondo, M. J., Font, G., *J. Chromatogr. A* 1999, *839*, 101–107.

[18] Blasco, C., Picó, Y., Mañes, J., Font, G., *J. Chromatogr. A* 2002, *947*, 227–235.

[19] Wang, H., Yan, H., Qiao, J., *J. Sep. Sci.* 2012, *35*, 292–298.

[20] García de Llasera, M. P., Gómez-Almaraz, L., Vera-Avila, L. E., Peña-Alvarez, A., *J. Chromatogr. A* 2005, *1093*, 139–146.

[21] Karageorgou, E. G., Samanidou, V. F., *J. Sep. Sci.* 2010, *33*, 2862–2871.

[22] Sun, H., Qiao, F., Liu, G., Liang, S., *Anal. Chim. Acta* 2008, *625*, 154–159.

[23] Zhang, Q., Hong, B., Liu, J., Mu, G., Cong, H., Li, G., Cai, D., *J. Sep. Sci.* 2014, *37*, 1330–1336.

[24] Synaridou, M. E. S., Sakkas, V. A., Stalikas, C. D., Albanis, T. A., *J. Chromatogr. A* 2014, *1348*, 71–79.

[25] Shen, H.-Y., Zhu, Y., Wen, X.-E., , *Anal. Bioanal. Chem.* 2007, *387*, 2227–2237.

[26] Bai, S.-S., Li, Z., Zang, X.-H., Wang, C., Wang, Z., *Chin. J. Anal. Chem.* 2013, *41*, 1177–1182.

[27] Xiong, Z., Zhang, L., Zhang, R., Zhang, Y., Chen, J., Zhang, W., *J. Sep. Sci.* 2012, *35*, 2430–2437.

[28] Zhang, Q., Li, G., Xiao, X., *Talanta* 2015, *131*, 127–135.

[29] Hu, C., Jia, L., Liu, Q., Zhang, S., *J. Sep. Sci.* 2010, *33*, 2145–2152.

[30] Aguilar-Arteaga, K., Rodriguez, J. A., Barrado, E., *Anal. Chim. Acta* 2010, *674*, 157–165.

[31] Xie, L., Jiang, R., Zhu, F., Liu, H., Ouyang, G., *Anal. Bioanal. Chem.* 2014, *406*, 377–399.

[32] Lia, Y.-F., Qiao, L.-Q., Li, F.-W., Ding, Y., Yang, Z.-J., Wang, M.-L., *J. Chromatogr. A* 2014, *1361*, 77–87.

[33] Dados, A., Paparizou, E., Eleftheriou, P., Papastephanou, C., Stalikas, C. D., *Talanta* 2014, *121*, 127–135.

[34] European Commission Health & Consumer protection Directorate-General, Guidance document on analytical quality control and validation procedures for pesticide residues analysis in food and feed, in: SANCO/12571/2013, European Commission Health & Consumer protection Directorate-General, November 2013.

